14160

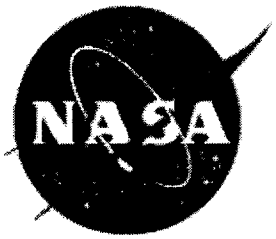

A Survey and Comparison of Several Space Shuttle External Tank (ET) Ice/Frost Detection and Evaluation Systems

Working Paper and Progress Report

Visual Perception Laboratory
US Army TARDEC
6501 East Eleven Mile
AMSRD-TAR-R/MS 263
Warren, MI

June 1, 2004

Submitted to: NASA as part of the NASA/TACOM Space Act Agreement (SAA)

Armando Oliu, Robert Speece and Ronald Phelps, NASA Kennedy Space Center (KSC)

Prepared by: Dr. Thomas Meitzler, Team Leader
Dr. Elena Bankowski, Dr. David Bednarz, Mary Bienkowski, Jennifer Bishop, Darryl Bryk, Kimberly Lane, EJ Sohn, John Vala, US Army TARDEC

Dr. James Ragusa, Consultant

Report Documentation Page

Form Approved
OMB No. 0704-0188

1. REPORT DATE	2. REPORT TYPE	3. DATES COVERED
29 JUN 2004	**N/A**	**-**

4. TITLE AND SUBTITLE	5a. CONTRACT NUMBER
A Survey and Comparison of Several Space Shuttle External Tank (ET) Ice/Frost Detection and Evaluation Systems Working Paper and Progress Report	5b. GRANT NUMBER
	5c. PROGRAM ELEMENT NUMBER
6. AUTHOR(S)	5d. PROJECT NUMBER
Meitzler, Dr. Thomas; Bankowski, Dr. Elena; Bednarz, Dr. David; Bienkowski, Mary; Bishop, Jennifer; Bryk, Darryl; Lane, Kimberly; Sohn, EJ; Vala, John Ragusa, Dr, James (Consultant)	5e. TASK NUMBER
	5f. WORK UNIT NUMBER
7. PERFORMING ORGANIZATION NAME(S) AND ADDRESS(ES)	8. PERFORMING ORGANIZATION REPORT NUMBER
USA TACOM 6501 E 11 Mile Road Warren, MI 48397-5008	**14160**
9. SPONSORING/MONITORING AGENCY NAME(S) AND ADDRESS(ES)	10. SPONSOR/MONITOR'S ACRONYM(S)
	TACOM TARDEC
	11. SPONSOR/MONITOR'S REPORT NUMBER(S)

12. DISTRIBUTION/AVAILABILITY STATEMENT

Approved for public release, distribution unlimited

13. SUPPLEMENTARY NOTES

Submitted to: NASA as part of the NASA/TACOM Space Act Agreement (SAA)

14. ABSTRACT

15. SUBJECT TERMS

16. SECURITY CLASSIFICATION OF:			17. LIMITATION OF ABSTRACT	18. NUMBER OF PAGES	19a. NAME OF RESPONSIBLE PERSON
a. REPORT	b. ABSTRACT	c. THIS PAGE			
unclassified	**unclassified**	**unclassified**	**SAR**	**45**	

Standard Form 298 (Rev. 8-98)
Prescribed by ANSI Std Z39-18

Table of Contents

Introduction....3

Objectives....3

Constraints....3

Mutual Benefits....4

Technical Background....4

Methodology....16

MD Robotics System....18

Ice Thickness Measurements....21

Density Measurements....25

Foam Swelling Tests and Determination....25

MD Robotics Data Analysis....29

Statistical Analysis....32

Goodrich Corporation IceHawk System....36

Preliminary Conclusions....40

Suggestions for Future Research....41

References....42

Appendix A: Abbreviations....43

Appendix B: Sensor Technology Websites....43

Appendix C: Ice Thickness Data....44

Appendix D: Figure of Fowler Height Meter....45

A Survey and Comparison of Several Space Shuttle External Tank (ET) Ice/Frost Detection and Evaluation Systems

Introduction

This working paper and progress report has been prepared as part of a National Aeronautics Space Agency (NASA)-Kennedy Space Center (KSC), Florida/U.S. Army Tank Automotive Research, Development & Engineering Center (TARDEC) Warren, Michigan Space Act Agreement (SAA) signed on 21 January 2004. This mutually-beneficial collaborative research investigation is being accomplished under the terms of a Statement of Work (SOW) entitled: "Ice/Frost Detection and Evaluation" jointly signed in March 2004 by Ronald Phelps of NASA-KSC's Shuttle Processing Business Office, and Dr. Thomas Meitzler of TARDEC's Visual Perception Lab (VPL). Planning and implementation has involved collaboration between U.S. Army investigators and NASA-KSC's Ice/Debris Team. Acronyms and abbreviations used in this report are included in Appendix A.

Objectives

The primary objectives of this joint research effort were to identify, investigate, and test commercially available sensor systems that have the potential to remotely detect and quantitatively measure ice formed on the insulated foam surface of the External Tank (ET) of NASA's Space Shuttle during pre-launch operations. The formation of ice (and frost), caused by ambient air condensation, is a common occurrence on the insulated ET holding cryogenics–in this case super cold liquid hydrogen and liquid oxygen. The reason ice is of critical concern is the possibility of formed ice breaking off of the ET during liftoff and vehicle assent, and subsequently striking and possibly damaging the Orbiter crew compartment windows placing the crew and vehicle at risk.

Constraints

In certain locations on the ET, pre-launch ice that exceeds a Launch Commit Criteria (LCC) ice thickness limit of $1/16^{th}$ (0.0625) of an inch (in.) and having a diameter of 1 in. or more are a significant constraint to launch[2] and can easily occur in the moist, warm Florida KSC launch complex environment. Also important for ice growth prediction purposes is the differentiation of frost and ice on ET foam surfaces. Launch pad inspection and qualitative assessment of frost and ice formation are possible during a planned launch minus 3-hour walk-down by the NASA Ice/Debris Team. During these walk-downs ice and frost presence can be detected, but not ice thickness because of the unavailability of a measurement tool and limited visual access to many external surfaces of the ET. Once the launch pad is cleared for the final phase of the launch countdown, ice and frost detection and monitoring are only possible using a remote sensor on the Rotating Service Structure (RSS), and another located at a perimeter road camera pad site--some 80 ft. and 1,200 ft. from the vehicle, respectively. However, even with these sensors, only a limited amount of surface area can be monitored.

While not presently a constraint, it is desirable to have only passive systems available for ice and frost remote detection and measurement. By definition "passive" means energy is not transmitted from the remote sensor--only received. "Active" means that the detection system transmits some form of electromagnetic energy to an area of interest. By mutual agreement

between NASA and the U.S. Army, it was decided that active systems would also be tested if a passive system could not be found. This was the case during this investigation.

Mutual Benefits

For NASA, the benefit of remote sensors that can detect and measure the presence and thickness of ice, and differentiate between frost vs. ice can make the difference between continuing or scrubbing a Space Shuttle launch countdown. Not only is a scrubbed launch expensive, but significant delays in a launch reschedule are likely because of limited "windows" of opportunity.

For the U.S. Army and other Department of Defense (DoD) service branches, both fixed-wing and rotary wing aircraft exist in their inventories. Ice detection on wings and rotors is critical since often these aircraft must function in extreme cold and ice-forming environments. Also, of great importance to the DoD are the capabilities for the remote detection and assessment of damage to vehicles and targets within a combat zone and identification of Friends-or Foes from a distance.

Technical Background

A governing document of the Space Shuttle Program (SSP), NSTS-07700 states that frozen water/moisture of 18 lb/ft^3 or higher is defined as ice. Any frozen moisture less than 18 lb/ft^3 is defined as frost. On the acreage of the ET anything from very light frost to ice of 18 lb/ ft^3 up to 37 lb/ ft^3 can form.[1] On the ET, the worst icing condition occurs in the Liquid Oxygen (LO2) feed-line bellows area. The overall design of the ET Thermal Protection System (TPS) foam minimizes ice formation on ET metal surfaces. Ice prevention on all protuberances of the shuttle ET is equivalent to that provided on ET cryogenic surfaces except for areas where, by design, the formation of ice cannot be prevented and has been accepted by the SSP. For example, the acceptance of this ice buildup is based on both engineering analysis and previous experience. The accepted ice areas are listed in Table 1 and range from 1 in^2 to 506 in^2, and are described by photographs included in section 2-1 of NASA NSTS No. 08303 on Ice/Debris Inspection Criteria [2].

For clarification and orientation for the reader, Figs. 1 through 7 (from selected areas of the NASA report NSTS 08303) show critical locations where ice and frost form on various parts of the Space Shuttle ET. Figures 8 through 15 show various areas of the ET and other relevant pictures that were obtained when members of TARDEC's VPL team visited NASA KSC in the summer of 2003.

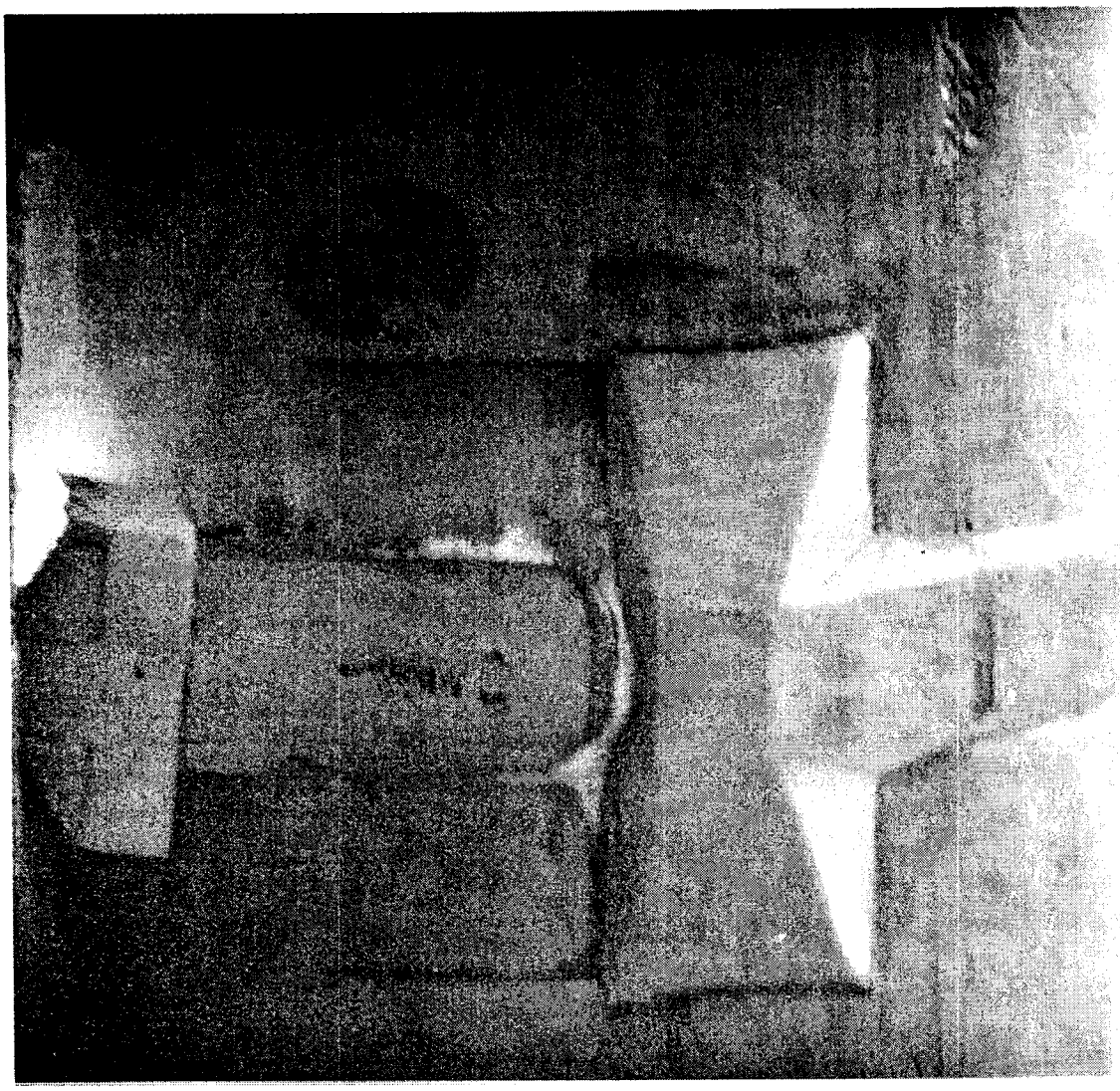

Fig. 1 Typical ice/frost formation, shown in white, on the inboard side of the LO2 feedline strut joints. This joint is designed to allow movement of the LO2 feedline support. The clearance between feedline parts does not permit the application of sufficient Spray-On Foam Insulation (SOFI) thickness to prevent the formation of ice/frost.

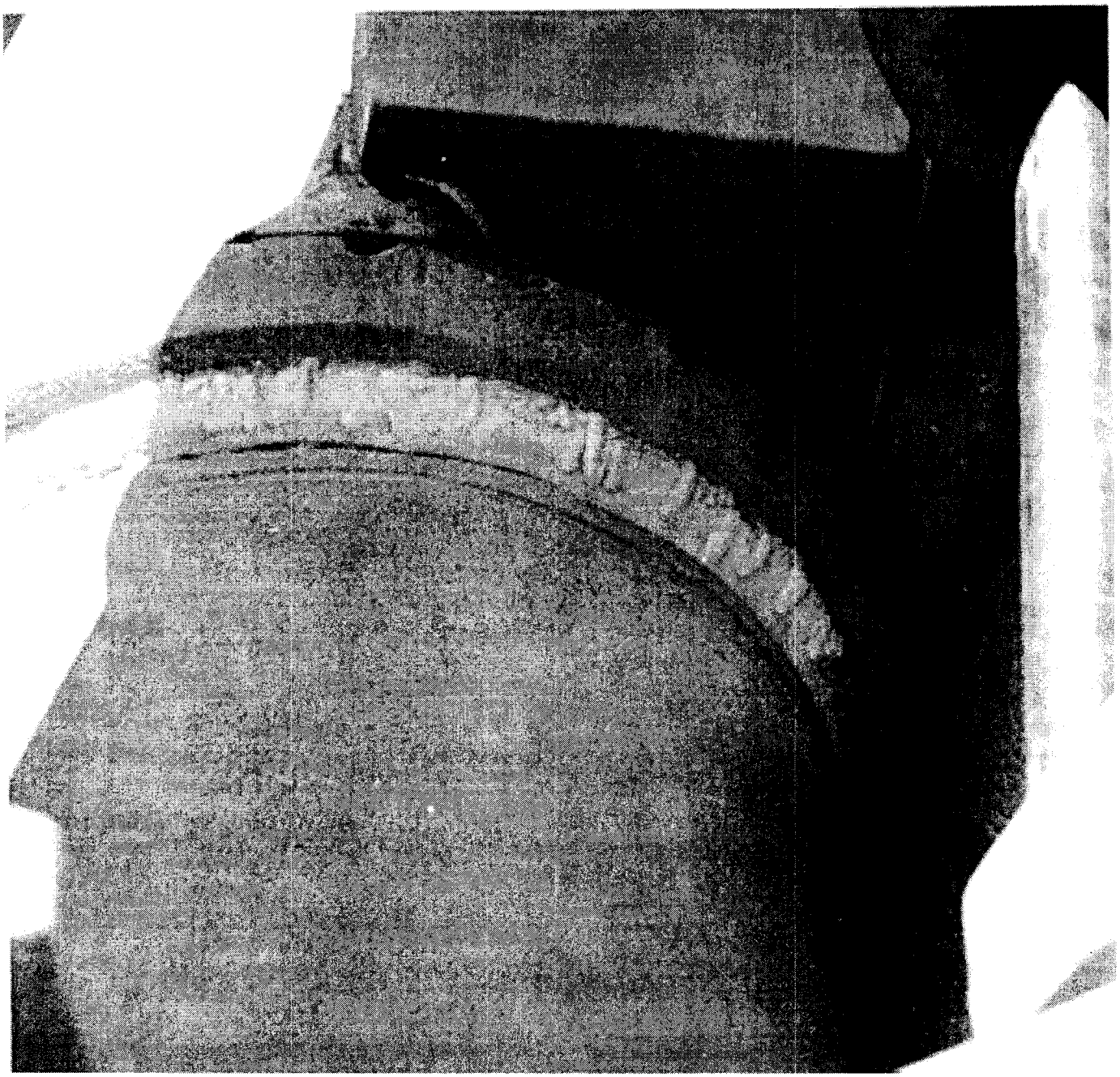

Fig. 2 Ice/frost formation in the LO2 feedline lower bellows at station XT–1978.8. The bellows are designed to allow feedline motion and are not covered by the Thermal Protection System (TPS). The ice/frost forms when moisture in the air contacts the cold surface of the bellows. Note ice/frost accumulation on the support bracket.

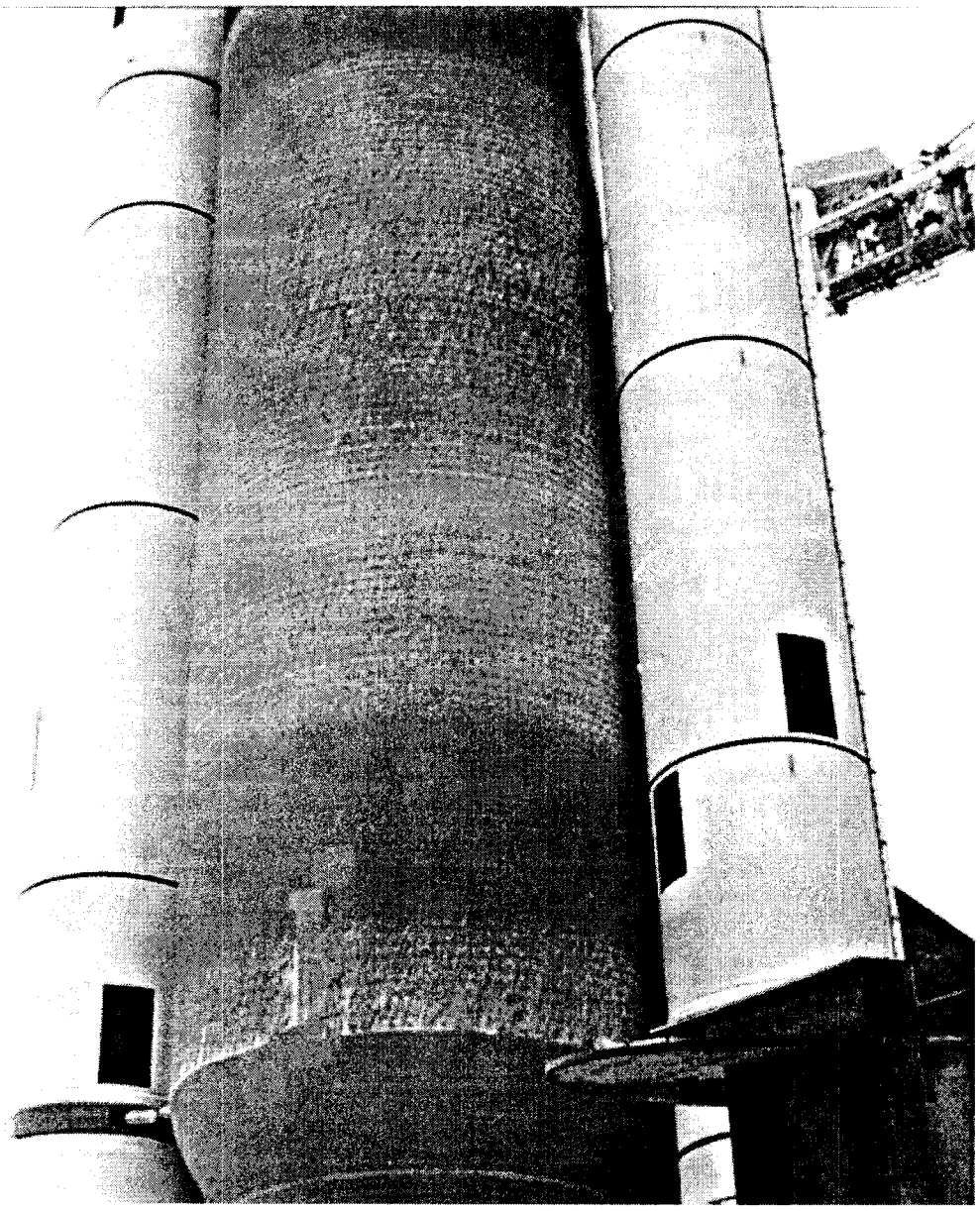

Fig. 3 Ice/frost accumulation on the –Z side of the ET was predicted by a NASA ice growth computer program to be 0.080 in. thick. Although the accumulation exceeded the LCC limit of 0.0625 in., it was acceptable for flight due to location in an allowable zone (–Z side) of the tank, (i,e, away from Space Shuttle windows).

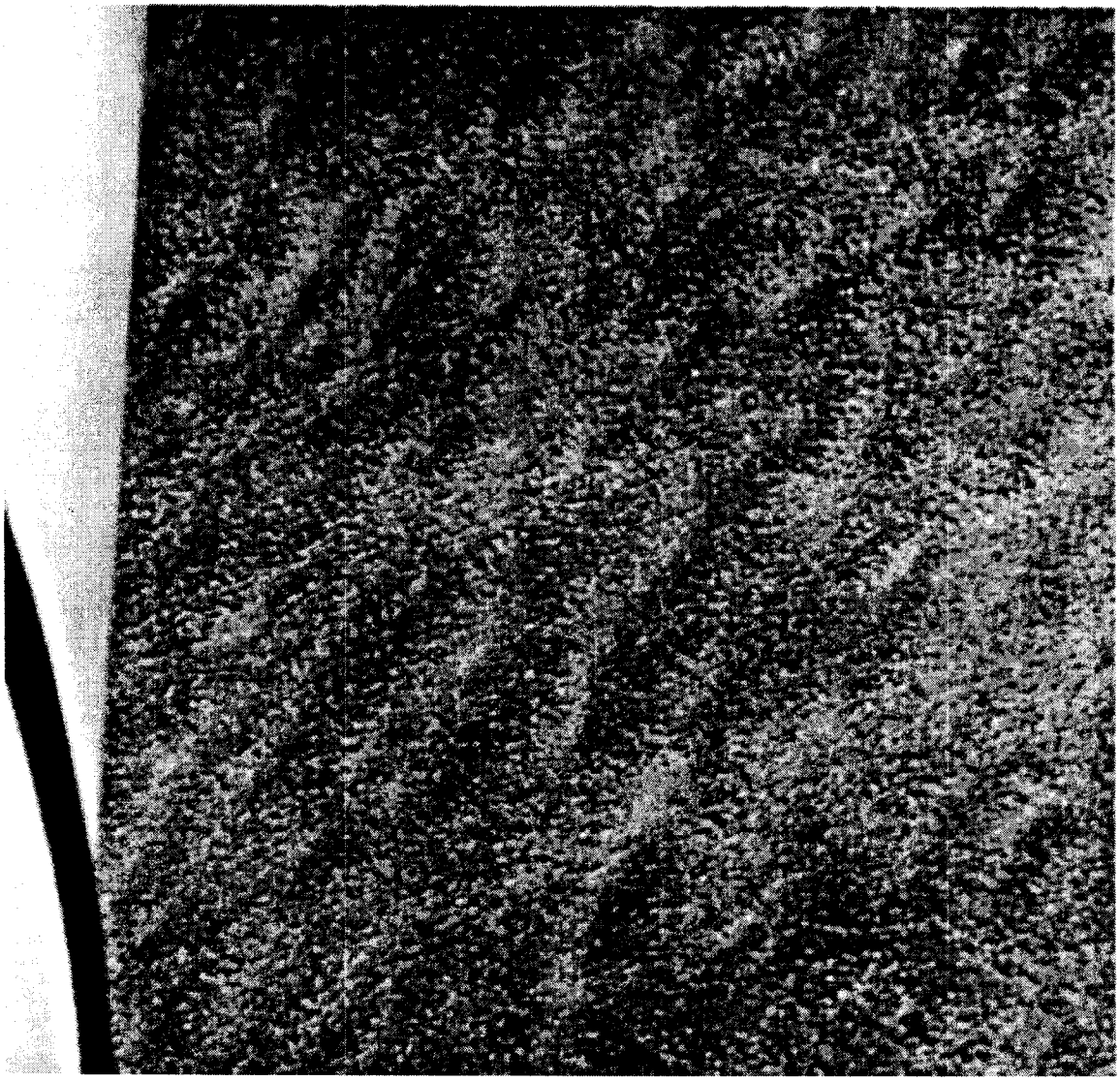

Fig. 4 Close–up view of ice/frost accumulation on the rough surface of ET acreage SOFI. The accumulation was less than 1/16th in. and acceptable per the LCC.

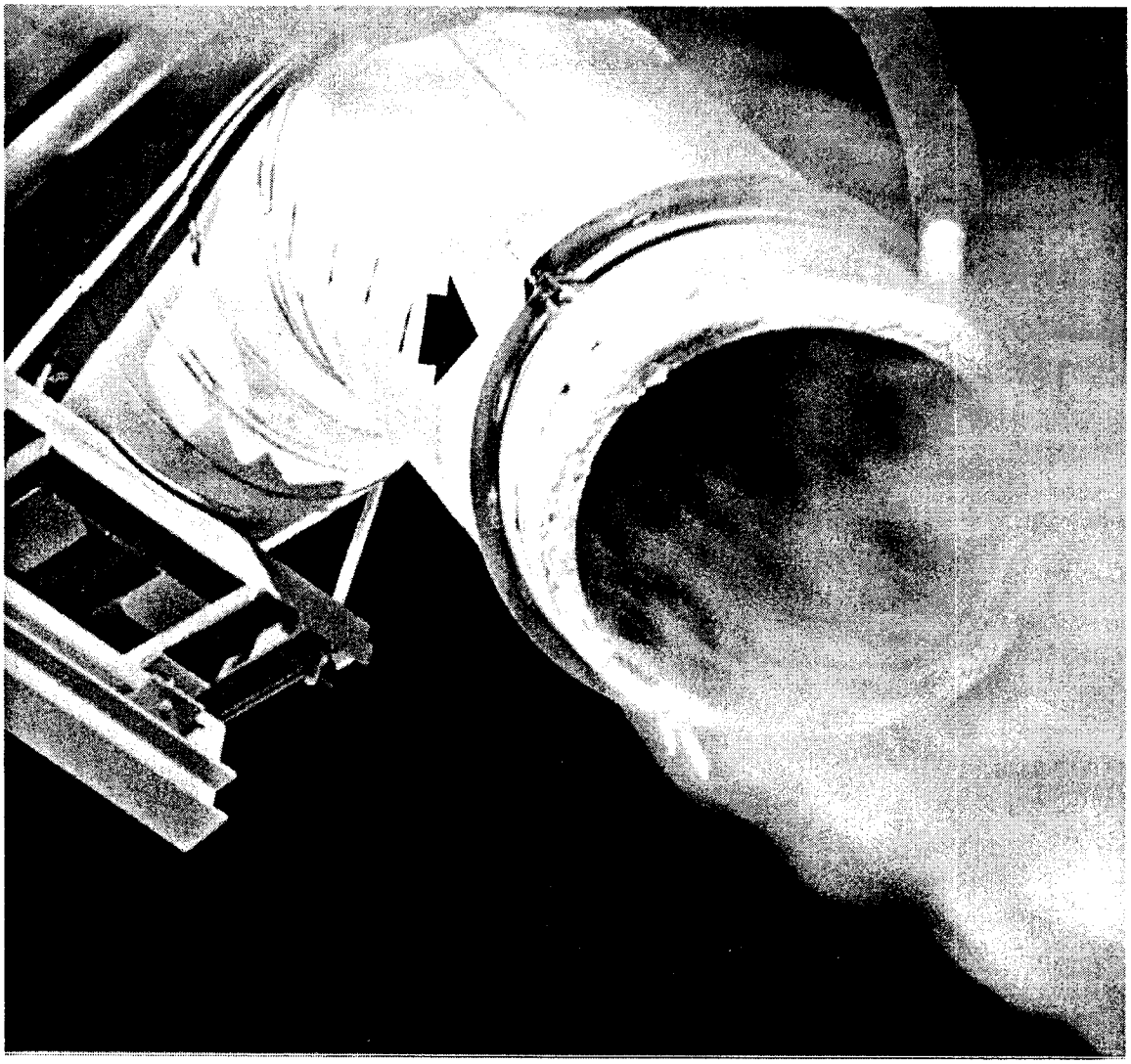

Fig. 5 Although hydro diverters were installed on the GOX vent ducts, conditions may still be right to form large icicles. Sheet ice or icicles on the GOX vent ducts are not normally acceptable for launch, but may be waived depending on wind conditions.

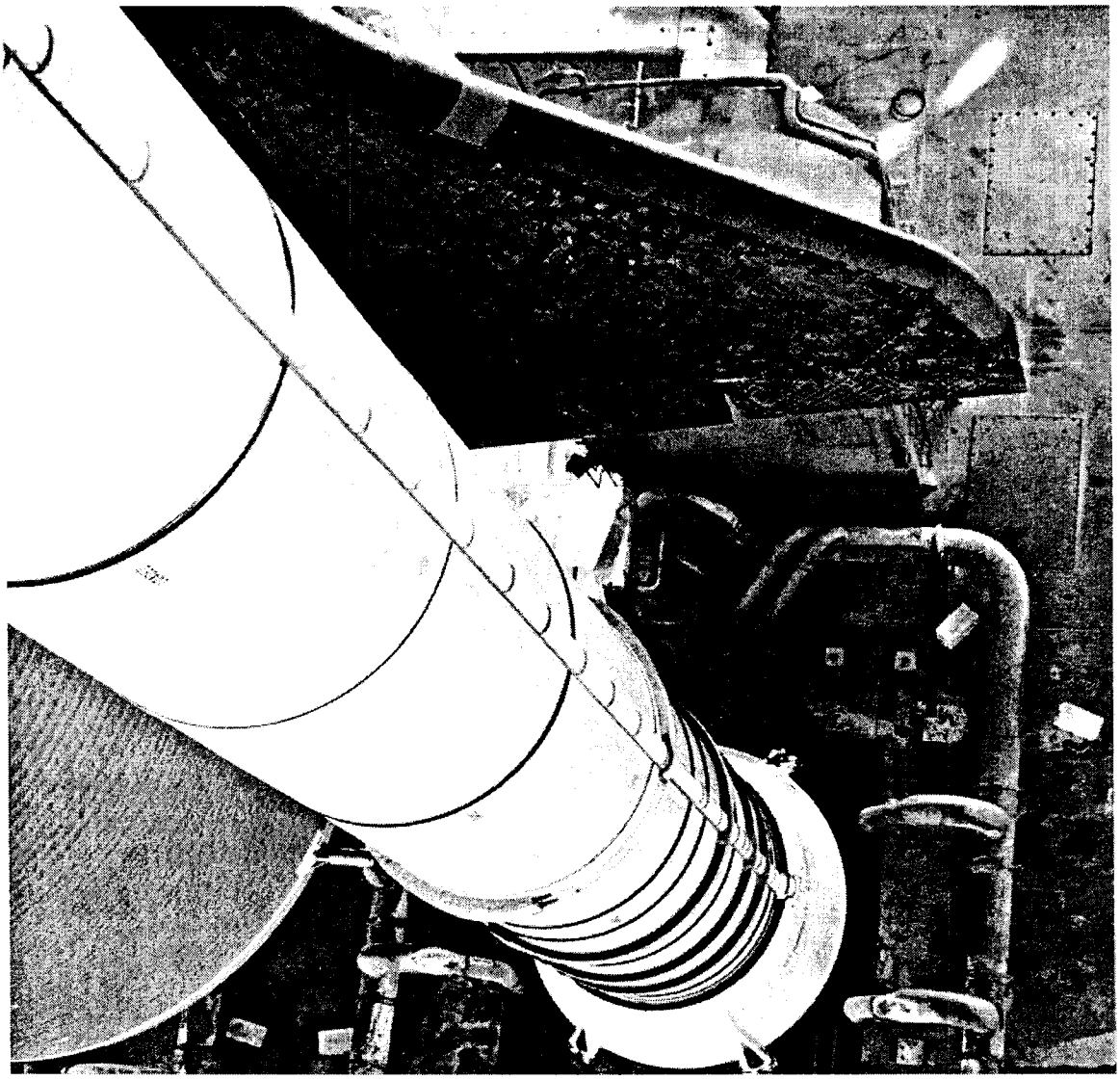

Fig. 6 View from GOX vent arm showing location on left hand Space Shuttle wing where lower surface tiles were damaged by icicles falling from GOX vent ducts.

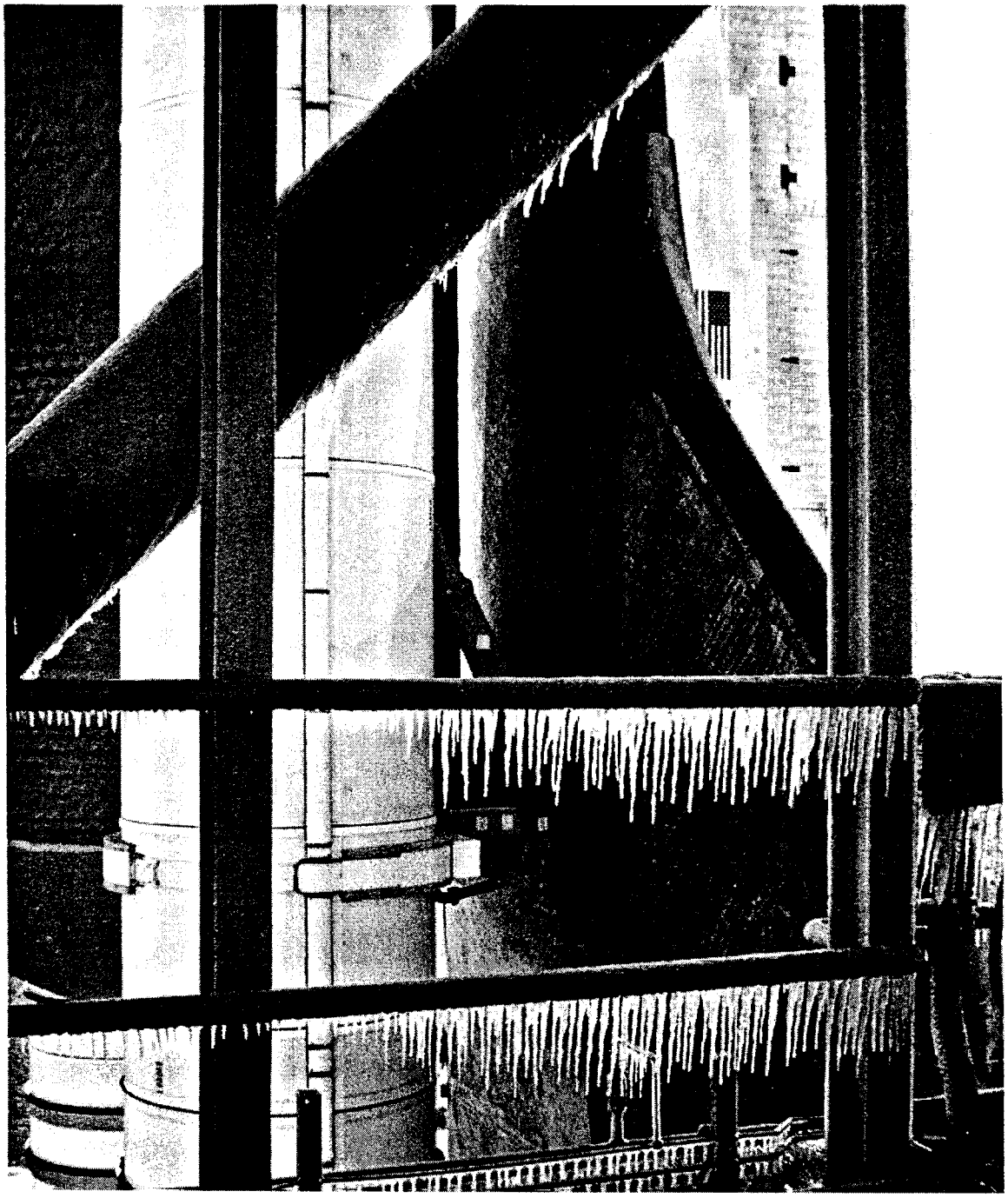

Fig. 7 Icicles/ice debris on the east side of the FSS can be drawn toward the vehicle by SRB and SSME plume aspiration and is not an acceptable condition for launch.

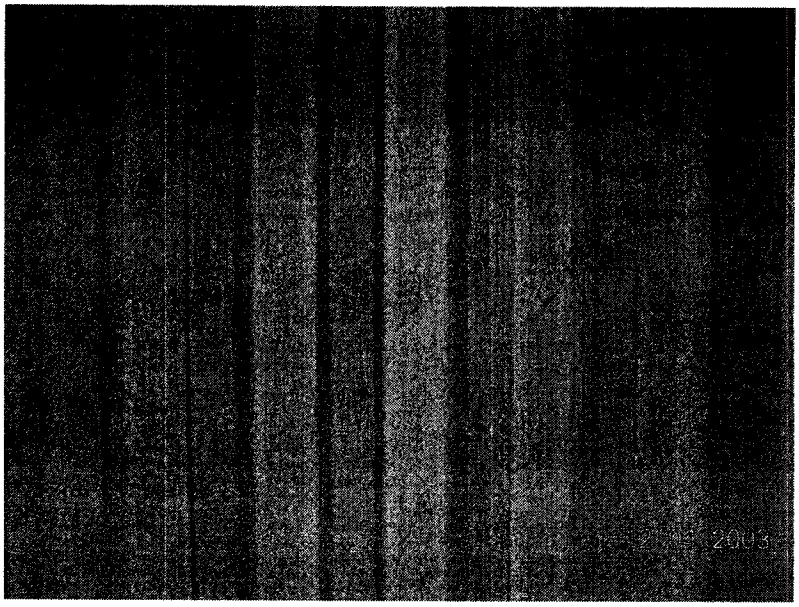

Fig. 8 Close-up of the machine-made corrugated foam surface of the ET

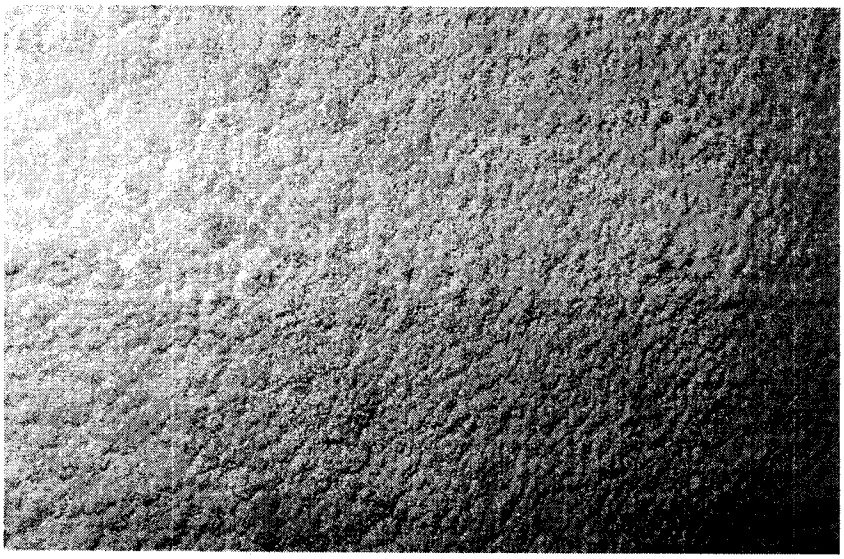

Fig. 9 Close-up of the variable height foam surface of the ET

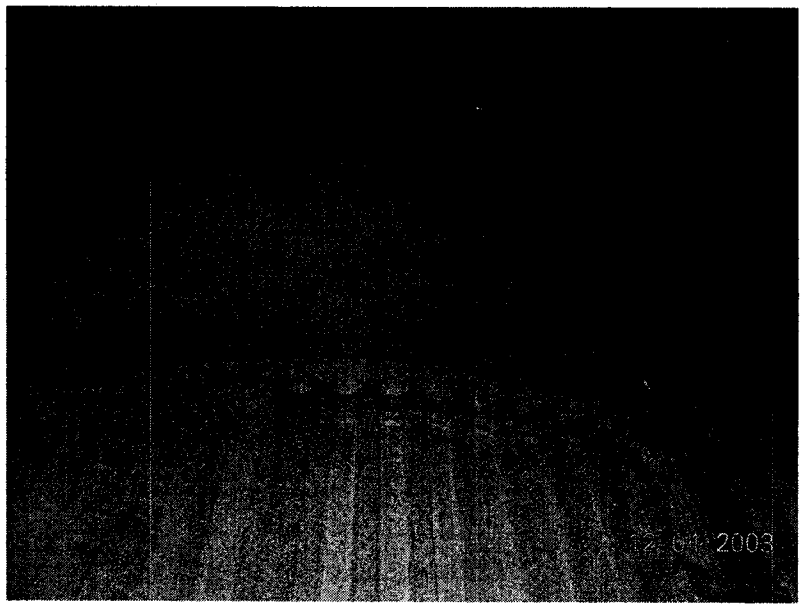

Fig. 10 Close-up of the ET from within the VAB on the upper level of the platform looking up at the ET LO2 storage tank

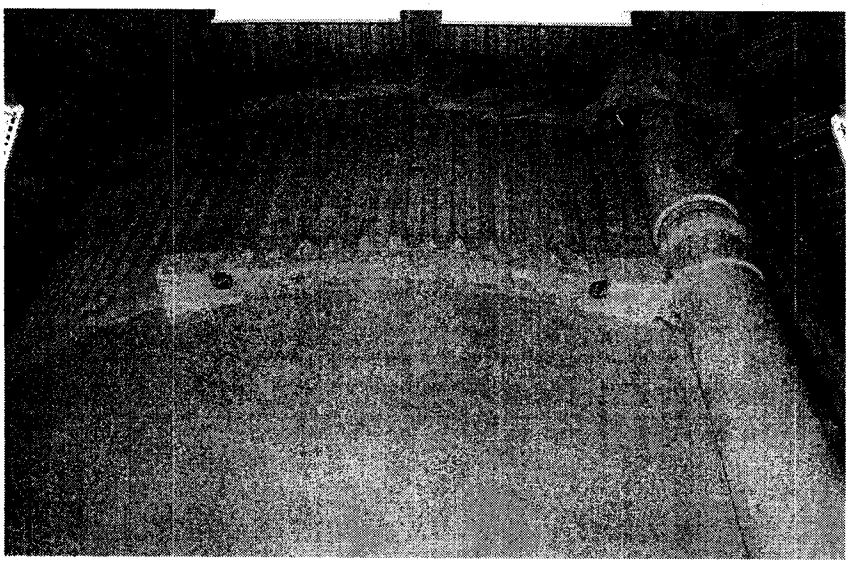

Fig. 11 Interstage area of the ET surface in VAB

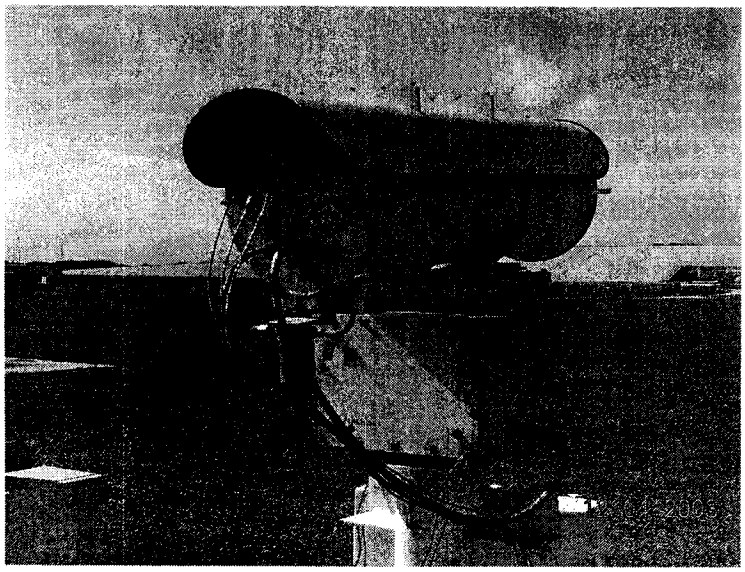

Fig. 12 IR sensor and housing located on the launch site perimeter road camera pad approximately 1,200 ft from the Space Shuttle vehicle

Fig. 13 Ice/Debris Team Leader Armando Oliu describes a feature of the ET surface to Dr. Tom Meitzler

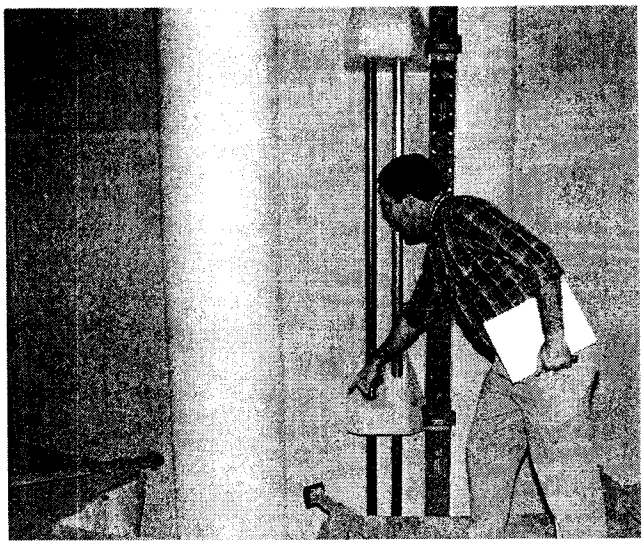

Fig. 14 Engineer Bob Speece describes an area of the ET

Fig. 15 Starting from the left: Dr. James Ragusa, Consultant; from TARDEC Ed Recke, Steven Schehr, Dr. Grace Bochenek, Dr. Thomas Meitzler, and Ron Phelps, NASA-KSC in front of pad A.

Methodology

Preliminary ice presence and thickness measurements were made using a low-power active laser method [3] identified from a research literature search, and through the use of a passive infrared (IR) radiometric imager. For initial test purposes, the laser used was a low-power red laser pointer like ones used in lectures. An internally calibrated radiometric IR camera forms an image of the scene, and specifically determines a temperature of each area in the scene based on its thermal radiance.

Army researchers were initially encouraged at the apparent ability of a particular radiometric imager to detect ice. However, after some thought and discussion with NASA representatives, they became concerned that this method of measurement could give ambiguous readings. The reason being that the presence of a cold region at the same temperature of ice was being detected instead of the ice itself. For reference, Table 1 shows values of accepted ice tolerances on the ET.

Table 1 Ice Tolerances for the ET

ITEM	DESCRIPTION	XT	YT	ZT	MAX. ICE AREA
17 in LO2 feedline	Bellows Shield	1106	70	564	3 in sq.
		1978.8	70	564	3 in sq.
		2026.4	70	564	3 in sq.
	Supports	1129	70	564	258 in. sq.
		1377	70	564	286 in. sq.
		1623	70	564	280 in. sq.
		1871	70	564	175 in. sq.
		1973	70	564	150 in. sq.
	Flange at I/T	1115	70	564	27 in. sq.
	ECO Sensor Cond.	1623	70	564	13 in. sq.
LH2 Recirc. Line	Bellows Shield	2095	–66	587	6 in. sq.
		2108	–53	551	6 in. sq.
Exp. Instr./Purge Vents		2093	80	590	1 in. sq.
		2093	–80	590	1 in. sq.
Thrust Struts	Left at Tank	1927	–112	523	12 in. sq.
	Right at Tank	1027	112	523	12 in. sq.
ET/SRB aft Attach	Cable Tray	2058	–157	471.94	40 in. sq.
		2058	157	471.94	40 in. sq.
	Diagonal Strut	2058	165.87	443.22	134 in. sq.
		2058	165.87	443.22	134 in. sq.
	Upper Strut	2058	173.29	457	506 in. sq.
		2058	173.29	457	506 in. sq.
TSE (shipping Flange)	Diagonal Strut	2058	26.44	558.44	20 in. sq.
Bipod Spindle	Right Hand	1129.9	42.7	564	6 in. sq.
	Left Hand	1129.9	42.7	564	6 in. sq.
LH2 aft Manhole	Upper Lk CK Port	2171	–4.8	412.6	9.6 in. sq.
	Lower Lk CK Port	2165	–4.8	340.1	9.6 in. sq.
LO2 Cable Tray at		2058	96.5	564.3	15.5 in. sq.
Torque Multiplier					
LO2 Feedline Bracket		2051	80	583	100 in. sq.

The physical principle behind a low power laser measurement system is illustrated in Fig. 16[3]. The experimental apparatus is shown in Fig. 17. In the latter figure, the laser pointer is held above the sample of ice at a distance of approximately one foot. By using clear ice, a dark interference ring can be seen and measured. (Ref. Fig. 18). This patented approach is of continued interest and should be further investigated and tested.

A laser beam of any visible wavelength or infrared wavelength outside the absorption band of ice can be used for testing purposes. In the Army Visual Perception Lab, investigators used a standard red laser pointer pen--the source with the best-formed beam of the ones tested. An optical aperture was used to reduce the beam diameter. As Fig. 16 illustrates, the laser beam was directed at the ice surface. *Importantly, the angle of beam incidence is not a factor to making this effect work.* In operation, the laser beam propagates through the ice and hits the diffuse underlying surface forming a bright spot from which light scatters in all directions. The light scattered from this spot and incident at the ice/air interface, at an angle less than the critical angle, gets transmitted through the ice/air interface. Light that strikes at angles greater than the critical angle is reflected back into the ice and strikes the rough surface below. The view perpendicular to the surface, as shown in Fig. 18, shows a bright spot where the laser initially strikes the surface surrounded by a dark annulus with a bright perimeter of diameter, D. The luminance of the brighter ring decreases in intensity as the distance from the center increases. At viewing angles other than normal, an ellipse is seen. The thickness of ice (H) is given by equations (1) and (2) that follow.

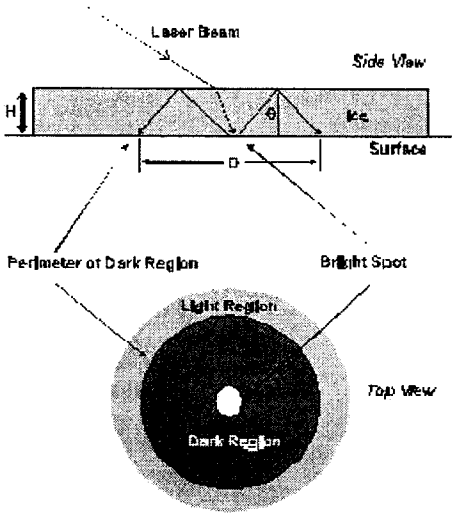

Fig. 16 Optical principle of laser method

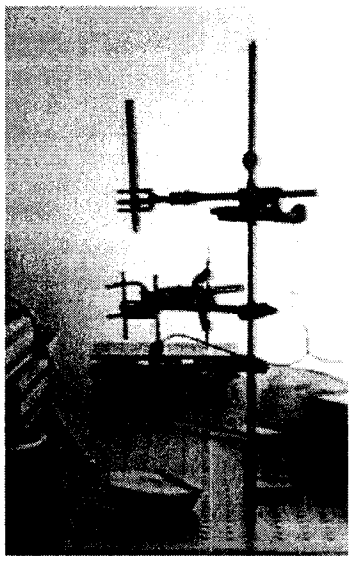

Fig. 17 Setup to verify method

$$H = \frac{D}{4 \tan(\theta)} \qquad (1)$$

where

$$\theta = \sin^{-1}\left(\frac{1}{n}\right) \qquad (2)$$

In Fig. 16, theta (θ) is the angle of incidence defined as the angle between the normal to the surface and the refracted beam--in this case approximately 50 deg. for water ice. The index of refraction is identified as n. It was found by VPL investigators that this technique works well, though only for clear ice or water with a light colored background. [3]

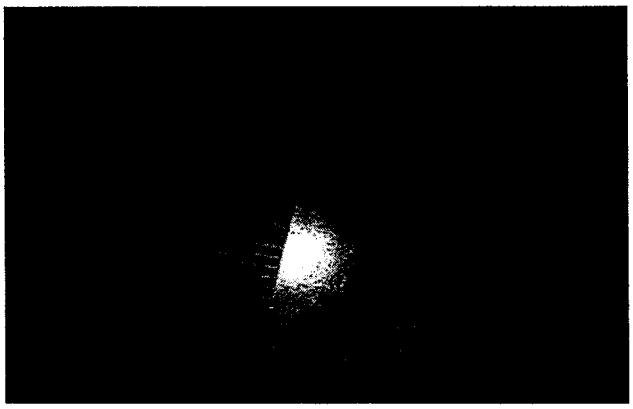

Fig. 18 Optical Ring seen through ice with ruler

Commercial Systems

Two commercially available active systems were tested for ice detection and measurement capabilities. They were: a system by MD Robotics, and the IceHawk system by the Goodrich Corporation. There were no passive systems found, and the active systems tested were the only ones available during this investigation.

MD Robotics System

A near IR camera system designed by MD Robotics of Canada capable of measuring ice thickness was identified in an Internet search of ice detection technologies. MD Robotics is a Brampton, Ontario, Canada company well known for space-borne and -based robotic arms and systems such as Canadarm that is used in the Space Shuttle payload bay, and the International Space Station's Canadarm2, Mobile Base System, and the Special Purpose Dexterous Manipulator. The company was contacted to perform an ice detection system demonstration and experimental trial in the VPL at TARDEC early in 2004. The system uses a 60-100 watt near-infrared strobe lamp to irradiate the ice sample from a specific distance. Keying off the absorption of infrared energy by ice, images are formed that are related to the computed thickness of ice. In operation, the returned optical signal is processed by algorithms and a computer to determine ice thickness. In the following images, the measured thickness of ice is color-coded from black to red corresponding to an ice thickness that can vary from 0 to greater than 0.53 in.

Several representative ET foam samples were fabricated and provided by NASA to Army VPL researchers for ice detection testing. To begin experimental work, a 13.7 ft^3 freezer was purchased by TARDEC, and leveled to achieve proper ice thickness formation. Each foam sample was numbered for identification and the upward direction identified with a permanent marker. Ice was formed on the samples by laying them face down (outward side down) in

square Teflon coated baking pans (approximately 7½ in. x 7½ in.). Weights were placed on the samples to prevent them from floating when water was poured into the pan. For some samples, ice thickness was controlled by mechanically elevating the foam above the bottom of the pan (more details below). The result was a flat and regular ice surface. Importantly, this controlled method of ice formation provided a way to measure ice thickness. Since the backs of the foam substrates were flat and clear of ice, ice thickness could be accurately determined by comparing obtained before and after ice formation measurements.

Sample Descriptions

A detailed description of each of the samples that were used for the tests are as follows:

Sample No. 1: A ramp of ice that varied from $^{1}/_{16}$ to ¼ inches. Three holes were drilled through the ET foam and an backing plate was then threaded for 6-32 machine screws, to elevate the foam face above the pan bottom at an angle. At one end of the sample, the screws were used to elevate the foam face by approximately $^{1}/_{16}$ in., and at the other end the height was set for ¼ in. A height gauge was used to measure ice thickness. Weight was applied to prevent floating, water added, and the sample was placed in the freezer.

Sample No. 2: A molded step of ice that varied from $^{1}/_{32}$ to ¼ in. A milled piece of aluminum was prepared with a set of five milled steps as shown in the drawing below (Fig. 19). The ET foam sample was laid face down over this milled aluminum form, a weight was applied to prevent floating, and water was added. Once frozen, the milled aluminum form was freed from the ice by chipping away excess ice, and removing the foam in such a way as to minimize damage to the ice sample.

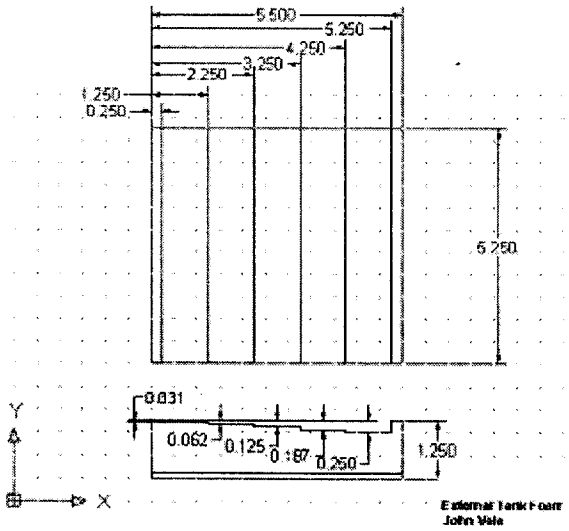

Fig. 19 Drawing of milled sample

Sample No. 3: Metal nuts, $^{3}/_{16}$ in. thick, were set between the pan bottom and the ET foam face to set ice thickness. This gave investigators an approximately $^{3}/_{16}$ in. thick sheet of ice over one entire foam sample face.

Sample No. 4: Not used.

Sample No. 5: This ET foam sample had approximately $^{1}/_{8}$ in. of snow pressed flat onto one surface. Snow was used in an attempt to create low-density ice.

Sample No. 6: Not used.

Sample No. 7: Milled steps of the ET foam. This ET foam sample was machined according to the same pattern as shown above for the Sample 2 aluminum form. This sample was placed face down and in direct contact with the pan bottom and frozen in water. The result was a smooth flat surface of ice on a foam sample with varying steps of foam thickness.

Sample No. 8: Step form molded snow applied to milled flat ET foam. This sample had the original foam surface milled off providing a flat smooth surface of foam. Snow was applied to the surface and formed into steps by firmly pressing the aluminum form, mentioned above, over it.

Sample No. 9: Step form molded snow. Snow was applied to the variable height ET foam surface and formed into steps by firmly pressing the aluminum form over it.

Sample No. 10: Approximately ¼-½ in. layer of snow was pressed flat onto the ET foam surface.

Sample No. 11: Painted $^{1}/_{16}$ in. metal washers in ice. This foam ET sample was spray-painted a light brown color (for the Goodrich IceHawk ice detection system). Approximately $^{1}/_{16}$ in. thick metal washers were placed between the foam face and pan bottom, and then water was added to make ice. This sample later had three holes drilled and tapped for screws (as in sample 1 above) to form a ramp of ice from $^{1}/_{16}$ to ¼ in. thick for testing of the IceHawk system described later in this report.

Importantly it must be mentioned that the ET foam external surface (the exposed side away from the ET metal structure) is convoluted (in this case "bumpy" with foam peaks and valleys). See Figs. 4, 9 and 26. For this reason, ice thickness values were averaged using measurements taken from near the four corners and from the center of the sample. Unfortunately and critical to this investigation, the variance in the height of ET foam surface "bumps" is of the same order of magnitude as the LCC ice thickness limitation–1/16th (0.0625) of an inch.

NASA NSTS-07700 identifies ice densities of 18-37 lb/ft^3. Typical ice is about 57 lb/ft^3. While VPL researchers were considering how to create low-density ice (i.e. < 37 lb/ft^3), one of the last snowfalls of the Warren winter occurred in March and the week before a planned

MD Robotics second test period. In anticipation of the need for low-density ice samples for the tests, a container was placed outside the VPL and snow collected. For Samples 8 and 9, collected snow was applied by hand to ET foam surfaces. For Samples 5, 8, 9 and 10 collected snow was applied to various surface shapes for low density simulated ice testing, (reference Sample descriptions).

First Series of Test Measurements

At the time of the first MD Robotics system test on 10 February 2004, the wrong lens was used so the system was not properly focused at the planned camera-to-samples distance of 10 ft. The camera and lens was configured for operation at a range greater than 15 ft. The close proximity of the samples produced unfocused camera images, which affected the accuracy of the thickness estimate within the framed portions of the samples. Regardless, ice thickness test results that varied from zero to greater than 0.53 in. were color-coded from black to red, respectively. For this testing, thickness measurements were taken using a manual caliper.

Images of the ice-covered ET foam samples were obtained using a Kodak DC265 digital camera. A sample image is shown below in Fig. 20. The corresponding calibrated infrared image that is output from the MD Robotics camera is shown in Fig. 21.

Fig. 20 Samples 3 and 2

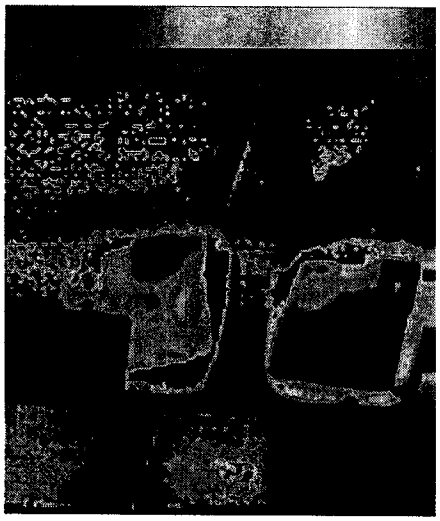

Fig. 21 Samples 3 and 2 with ice thickness color code

Table 2 shows the caliper measurements of ice thickness on ET foam (columns two to four), and MD Robotics camera measurements (column five) for the first MD Robotics test on 10 February 2004. Absolute and relative differences in the measurements are listed in columns six and seven, respectively. Fig. 22 shows the graph of the caliper measurements of ice on ET foam and MD Robotics camera measurements. It should be noted that the MD Robotics data might not be fully valid because of earlier noted lens problems during the February test. However, the data have been included in this progress report for completeness.

Table 2 The caliper measurements of ice thickness on foam and MD Robotics camera measurements

Sample #	Caliper (D)			MD Robotics Camera (d)	Absolute Difference	Relative Difference
	mm	inches	inches	inches	Abs[D - d]	Abs[D-d]/D
1	16.00	0.63	(5/8)"	No data		
2	3.00	0.12	(1/8)"	0.25	0.13	111.67%
3	3.25	0.13	(1/8)"	0.2	0.07	56.31%
3 middle	4.50	0.18		0.2	0.02	12.89%
3 right side	8.00	0.31		0.3	0.01	4.75%
4	4.50	0.18	(3/16)"	0.27	0.09	52.40%
5	9.00	0.35	(3/8)"	0.35	0.00	1.22%
5 bottom	8.00	0.31		0.3	0.01	4.75%
6	3.00	0.12	(1/8)"	0.22	0.10	86.27%
6 edges		1.10		0.3	0.80	72.73%
7	14.00	0.55	(9/16)"	0.3	0.25	45.57%
7 middle	12.50	0.49		0.5	0.01	1.60%
8	7.75	0.31	(5/16)"	0.3	0.01	1.68%
9	12.00	0.47	(15/32)"	No data		
10	3.25	0.13	(1/8)"	0.15	0.02	17.23%

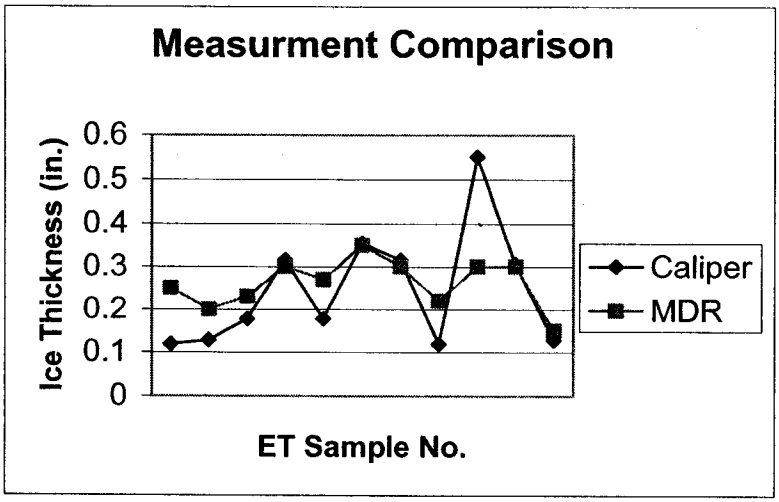

Fig. 22 Caliper measurements of ice on foam and MD Robotics camera measurements

Second Series of Test Measurements

MD Robotics representatives visited TARDEC for a second series of system tests on 23 March 2004. For that testing, a piece of plywood was set on an easel on which samples were hung or propped up on edge. As in the first test, the easel was place outside the VPL in approximately 35 deg. F weather. Samples were taken from the freezer, one or two at a time, and scanned individually with most of the foam sample filling the scan area. For identification in the scanned and photographed imagery, plastic numbers were hung near each ET foam sample. Data were taken and manually recorded in specific areas of each sample corresponding to similar areas where ice thickness had been (or would be later) measured (i.e., corner, center, and stepped areas). Manual measurements were changed from a caliper (used initially) to the Fowler precision gauge.

For this series of test measurements, a Fowler height gauge (see Appendix D) was used to measure ice thickness of the ET foam samples (instead of the caliper used earlier). Measurements were made on a precision flat optical table. The gauge consists of a precision rail and hand crank that raises or lowers a probe arm. Height readouts, from a digital LCD, were displayed to 1/1000 in. increments, and reading can be "zeroed" by pressing a reset button. By setting the zero position to the tabletop, the ET foam or ice sample's height above the table could be accurately measured by lowering the probe arm until contact was made. For samples that had hooks attached to their backing plates (for hanging up samples for ice detection scans) two precision 2 in. blocks were used for support.

Even during brief measurement periods, it was found that when the metal height gauge probe arm came into contact with ice an indentation was left. For that reason a new arm was fashioned out of metal stock and fitted with a hard rubber tip that provided more insulation and time to make undistorted measurements. The modified tip consisted of a hard rubber/plastic pad, with contact area approximately ½ x ½ in.^{2}, similar to the pads on the bottom of a computer case to prevent scratching of surfaces. (See Appendix D figure).

The samples were measured by laying them back-side down onto the optics table–or on 2 in. blocks if the sample had hooks. The height gauge was zeroed at the table base height or at the height of the blocks, and then several heights were recorded at selected positions (e.g. approximately ½ to 1 in. from each of the four corners, the center, or at each of the steps). The measurement locations were approximately the same regions before and after ice measurement. The measurements were made with and without ice so that the ice thickness was the only difference and variable of the two measurements. Since the foam surfaces are somewhat irregular ("bumpy"), the foam height is not totally accurate. The same is also true, of course, with any thickness measurements made by a remote sensing system.

The height gauge was operated manually by the crank handle, with some compression of the ET foam surface observed. It was estimated that height measurements could vary ± 0.05 in. depending on how much pressure was applied to the probe arm. Some variability was also found depending on who did the measurements. However, this error was assumed to be relatively small compared to the irregularity of the foam surface, and the resolution of the remote detection systems. Due to the variability of the foam surface and placement of the probe, it was estimated that measurements could be off as much as ±0.1 in.

Density Measurements

VPL investigators measured the density of some of the snow stored in the lab freezer. Measurements were taken in the Fuels and Lubricants building at TARDEC where Army investigators were given access to scales and graduated cylinders. The ice was transported in a cooler. The measurement of weights was facilitated using available and accurate lab scales. The first method of measuring snow volume was by submerging the ice in a fixed volume of water in a graduated cylinder and recording the water level difference made by the submerged ice. The snow was weighed on the scale prior to being submerged. Larger graduated cylinders have less gradations and accuracy, and since we had to have a large enough graduated cylinder to fit a piece of snow, the accuracy was limited (5 mL gradations). Also, this technique was lacking since submerging the samples in water fills in the air gaps, taking up some of the volume. VPL investigators tried a second method using a smaller graduated cylinder, with higher resolution (1 mL gradations). Crushed snow was lightly packed into the cylinder (not submerged in water) until a designated volume was reached, and then the sample was weighed. This measurement method proved more accurate. It was observed that the snow had mostly turned into ice after being in the freezer for about three weeks before the tests and therefore had probably increased in density.

Important to this investigation, the measurements obtained revealed that the snow (intended to represent low-density ice) was not as low density as was hoped. In fact the test samples were found to have an average density of about 52 lb/ft^3. These densities were higher than the worst icing conditions the ET experienced on the launch pad (as high as 37 lb/ft^3) where condensate ice was created. It is of merit to note that the MD Robotics engineers stated that the density of ice would not affect the accuracy of system predictions. This important system feature should be verified in a laboratory environment.

Foam Swelling Tests and Determination

It was observed by a representative from MD Robotics that their system is consistently 0.7 mm (.03 in) offset in thickness detection, and it was suggested that the foam could be swelling under water and/or ice conditions, as compared to their dry state and, thus affecting measurements. Although this is within our measurement error, to test this, Sample No. 8, which was milled flat foam, was measured for thickness, both dry and submerged in water (room temperature, not frozen). Sample No. 8 was used because it had been milled flat (rough surface removed) so it had a very uniform thickness to measure. Also, it was thought that with the rough surface removed more water may be absorbed through this non-weathered surface.

Dry Sample No. 8 was placed face-down into a Teflon pan. The Fowler gauge was zeroed for height at one corner. The gauge had to be modified with a metal extension in order to extend over the pan lip. The sample was then measured for thickness at the four corners of the sample. It was noted that the sample varied only slightly in thickness, to about 0.005 in. thicker at one corner. The sample was measured dry in the pan in order to cancel the height from the pan when subsequently measured with water. With a weight applied to prevent floating, water was added to the pan to a level just below the aluminum backing plate to maximize foam water absorption. The measurements were done again at the four corners and

appeared to not change appreciably (within measurement error–about .005 in.). The sample was left soaking in the water for about 3.5 hours and measured again with no appreciable differences.

To test any effect of swelling due to ice, Sample No. 5 (an unmodified ET foam sample) was chosen. The test plan was to measure a section of the ET foam, under dry and frozen conditions, to determine if it had expanded due to water absorption and ice formation. The sample thickness was measured dry and face-up at the southwest corner with the Fowler height gauge. The sample was then placed face down in water and placed in the lab freezer and left overnight--without any apparatus used to increase ice thickness. After removal from the freezer the next day, a thin irregular layer of ice on the sample face and in the rough foam valleys was observed. To prepare the frozen sample for measurement, a heat gun and paper towel were used to carefully remove the ice from the foam's southwest corner--the same corner that was measured in the dry state. The corner thickness measurement using the height gauge showed no appreciable difference beyond the typical error in repeated measurements (about 0.01in.). Since it took a little time to remove the ice from the corner surface (5-10 minutes), and some warming/melting had occurred, the sample was placed back in the freezer. After about an hour, the sample was removed from the freezer and again measured. Consistent with the earlier measurements, taken dry and frozen, no appreciable thickness differences were found. *As a result of these tests, although limited, a conclusion reached by Army VPL investigators was that the NASA-provided ET foam does not absorb enough water to measurably affect it's thickness*

Foam Ice Testing Results

Measurement of the ice thickness with the MD Robotics system was performed on Samples 1 through 11--this time using a correct focal length lens. Fig. 23 shows the MR Robotics camera system. There are two primary components, the near-IR strobe lamp on the right and the imaging camera on the left. A monitor and laptop computer were used to display the prediction thermographs. Fig. 24 shows the placement of the samples. Fig. 25 is the output processed image of the MD Robotics system with a color bar related to ice thickness. During the test that took place in the lab at TACOM, a prediction of the ice thickness, in numeric form, was displayed on a laptop computer. Test measurements and ice thickness values for tested samples are contained in Appendix C. Test results are graphically displayed in figures 28 through 32.

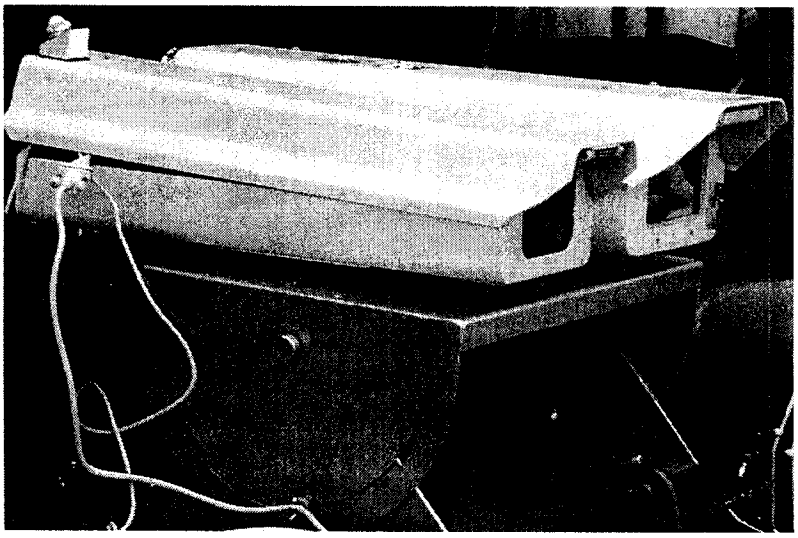

Fig. 23 MD Robotics System

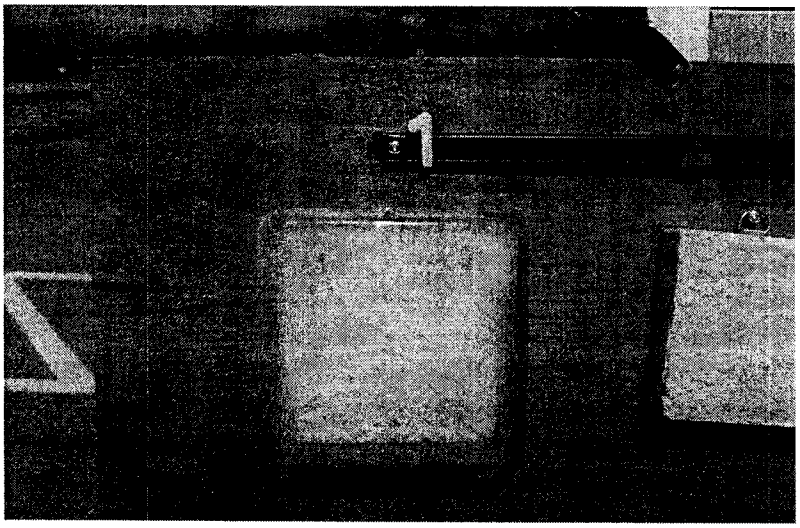

Fig. 24 Picture of ET Samples 1 and 2 with a thin ice layer

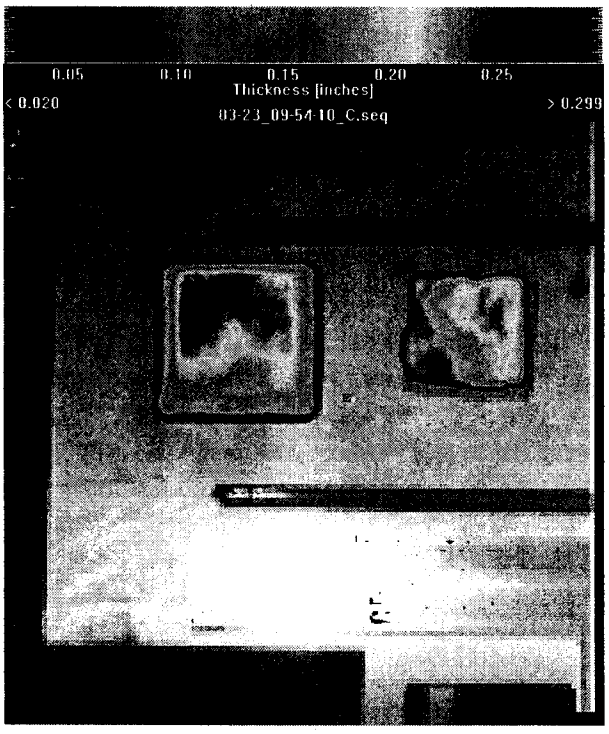

Fig. 25 Processed image of ice covered ET sample

Figures 26 and 27 are the visible and infrared MD Robotics system images, respectively, of Sample No. 2.

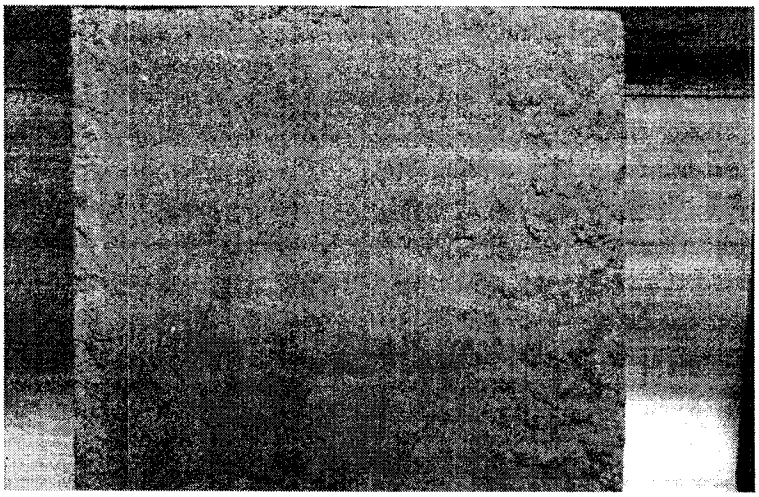

Fig. 26 Ice covered ET Sample No. 2 with graduated levels of ice

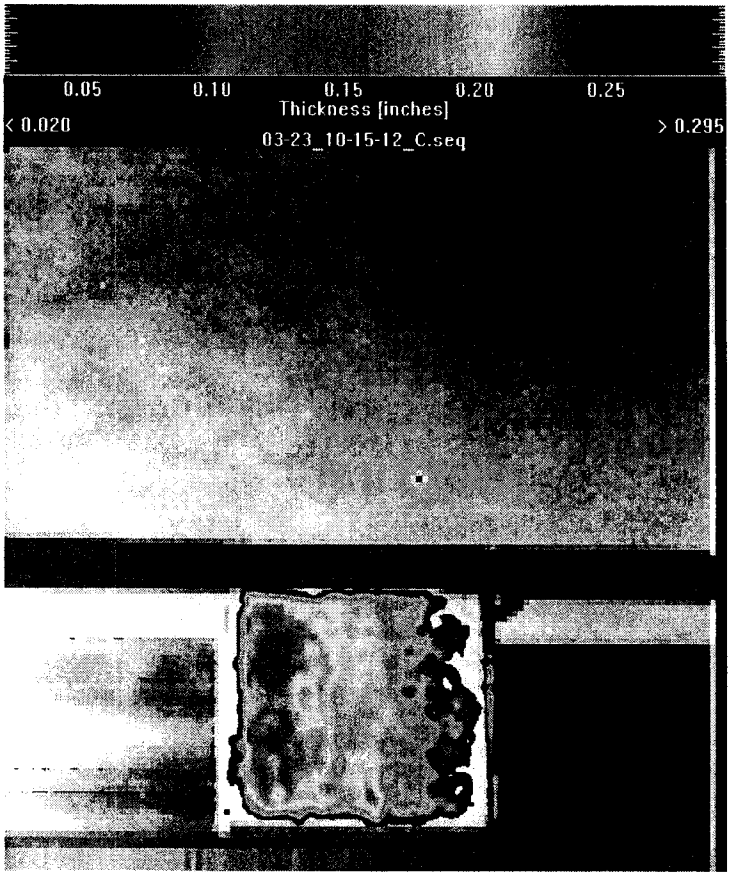

Fig. 27 MDR image of Sample No. 2 with graduated levels

MD Robotic Data Analysis

Figures 28 through 32 are graphs that show comparisons of the ice thickness of the samples as indicated by the MD Robotics system and measured by the Fowler height gauge. Error bars shown for MD Robotics reading are those recommended by the manufacturer.

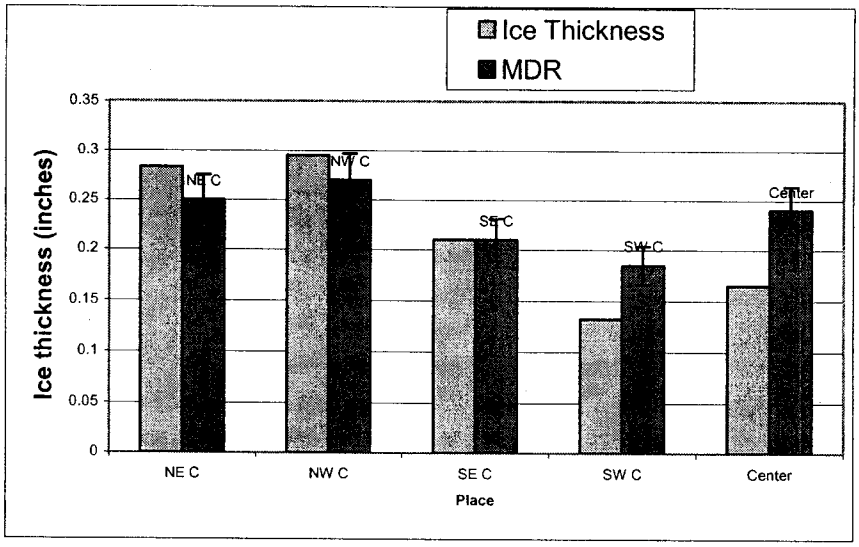

Fig. 28 Sample No. 1 thickness measurements

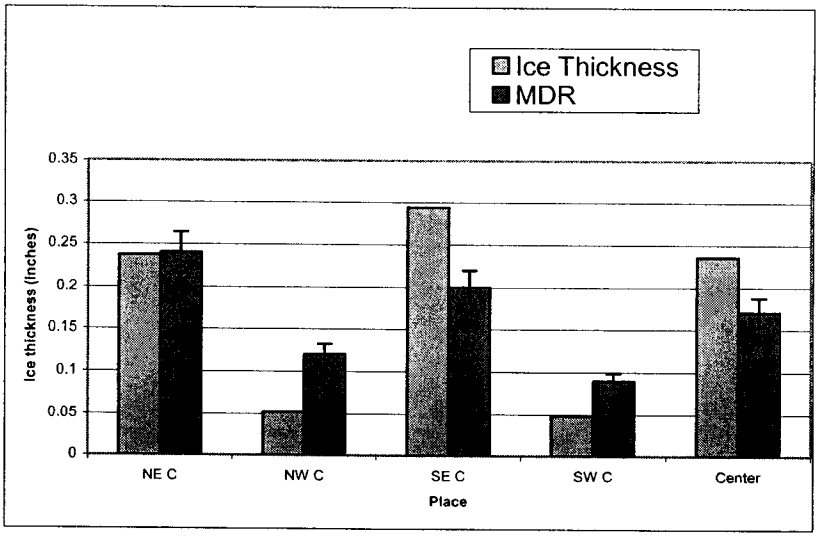

Fig. 29 Sample No. 2 thickness measurements

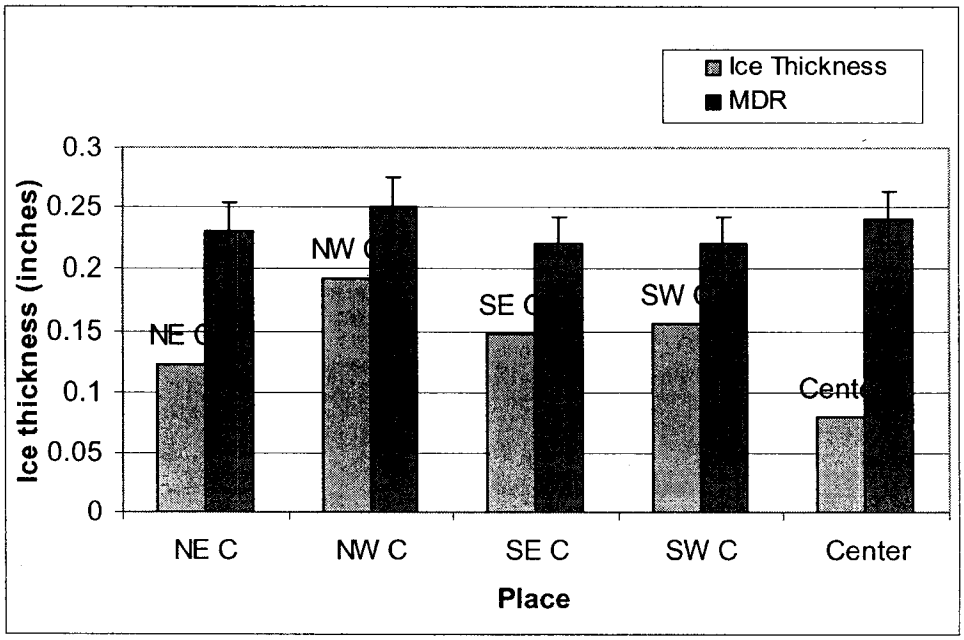

Fig. 30 Sample No. 3 thickness measurements

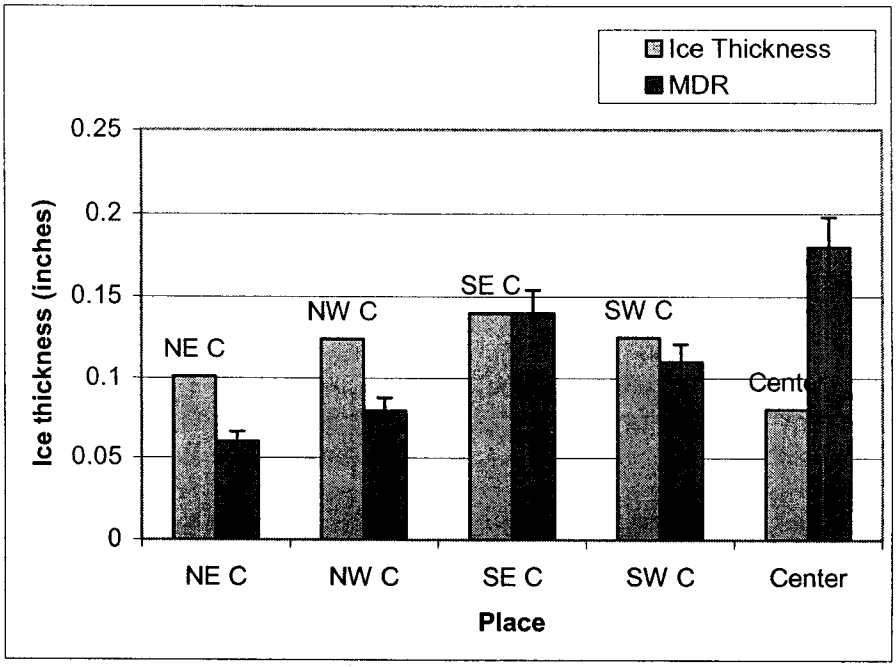

Fig. 31 Sample No. 5 thickness measurements

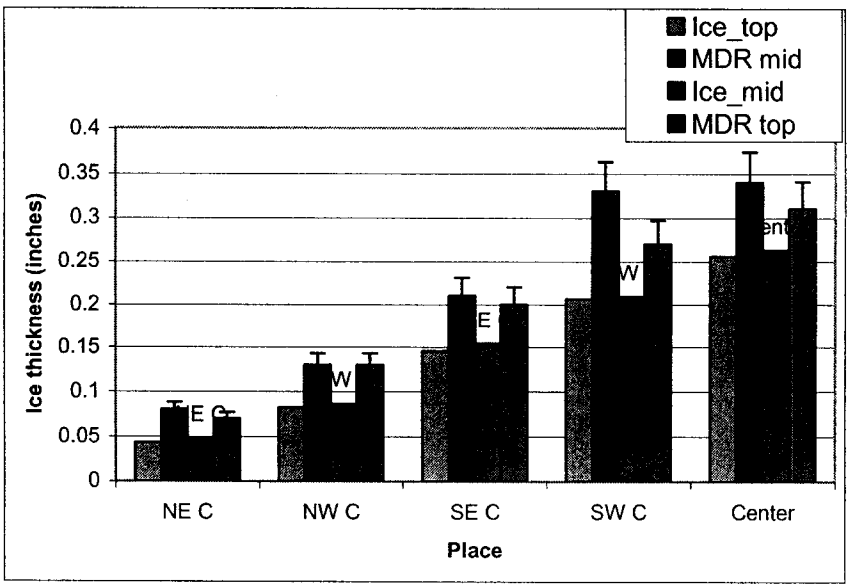

Fig. 32 Sample No. 7 thickness measurements

Statistical Analysis

The key question to be answered in this test sequence was whether the MD Robotics system produces similar readings of ice thickness as physical height gauge measurements. Since this test did not involve using a fixed set of foam samples with ice a certain ice thickness, a two-factor mixed model [5] was used where the two factors were the measuring device and the ice thickness. A mixed model was chosen because of the desire to make an inference about all possible measurements not just the particular samples that were tested. Since VPL investigators were interested in making conclusions about the entire population of foam samples, not just those used in the experiment, the foam sample is a random factor. The other factor, type of measuring device used, is a fixed factor. We now have the situation where one of the factors is fixed and the other is random. Thus, we have a mixed model analysis of variance. The experimental design for this experiment is a randomized complete random block design where,

$$y_{ij} = \mu + \tau_i + \beta_j + \varepsilon_{ij}\,. \tag{3}$$

In equation (3) the parameters are defined as follows:

μ = an overall mean
τ_i = fixed effect of the measuring device
β_i = the random block effect of the foam sample (4)
y_{ij} = ice thickness
ε_{ij} = normally distributed random error term.

Table 3 Tests of Between-Measuring Methods

Source		Type III Sum of Squares	df	Mean Square	F	Sig.
Intercept	Hypothesis	1.755	1	1.755	153.860	.000
	Error	.319	28	1.141E-02		
DEVICE	Hypothesis	2.202E-02	1	2.202E-02	12.807	.001
	Error	4.813E-02	28	1.719E-03		
SAMPLE	Hypothesis	.319	28	1.141E-02	6.636	.000
	Error	4.813E-02	28	1.719E-03		

The ANalysis Of VAriance (ANOVA) above in Table 3 shows that at the 1 percent level [5], the device type is significant, which means there is a statistically significant difference between hand operated gauge and the MD Robotics system measurements. This is determined by looking at the row labeled DEVICE in Table 3. The value of Sig is quite small. Thus, for any reasonable level of significance we will reject the null hypothesis of no difference in measuring devices.

It is important to check the adequacy of the assumed model and to check for potential problems with the normality assumption, unequal error variance by treatment or block, and block-treatment interaction. Residual analysis is the major tool used in diagnostic checking. A normal probability plot of the standardized residuals is shown in Fig. 33. There is no severe indication of nonnormality. Also, there is no evidence pointing to possible outliers. Fig. 34 is a detrended normal plot. If the sample is from a normal distribution the points should cluster in a horizontal band around zero. There should not be a pattern. This plot does not indicate any evidence of nonnormality. Fig. 35 and 36 give no indication of inequality of variance by treatment or block. Fig. 37 plots the standardized residuals versus fitted values. There should be no relationship between the size of the residuals and the fitted values.

In other words, the figures 33 through 37 show that the data fit to the model is good and that it is possible to state with confidence that there is significant difference between the hand operated gauge and the MD Robotics system measurements. Although the values between the hand operated gauge and the MD Robotics system are significantly different in value, the two measurement methods are strongly correlated as shown in Tables 4, 5, and 6.

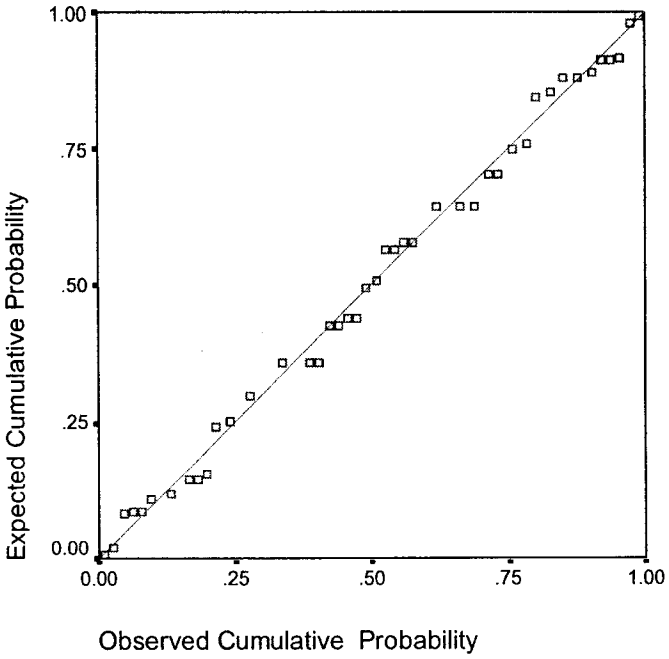

Fig. 33 Normal probability plot of standardized residuals

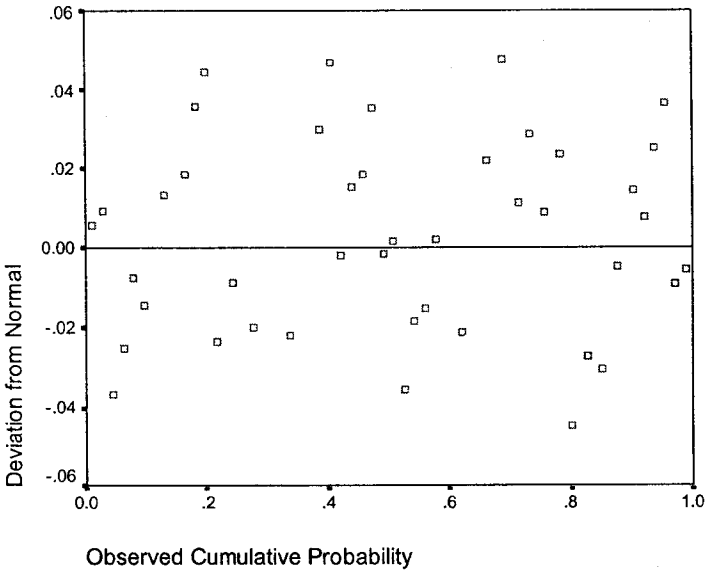

Fig. 34 De-trended plot of standardized residuals

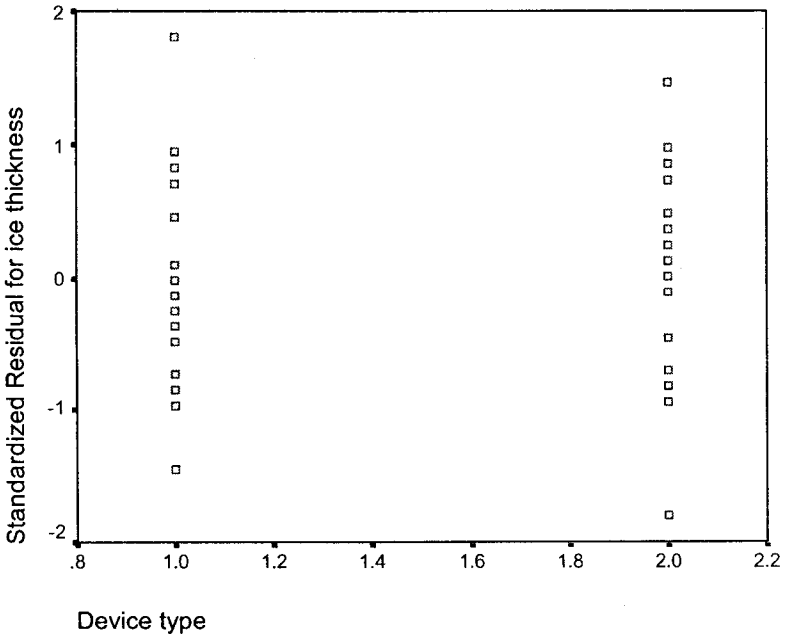

Fig. 35 Graph of standardized residuals versus measuring device type

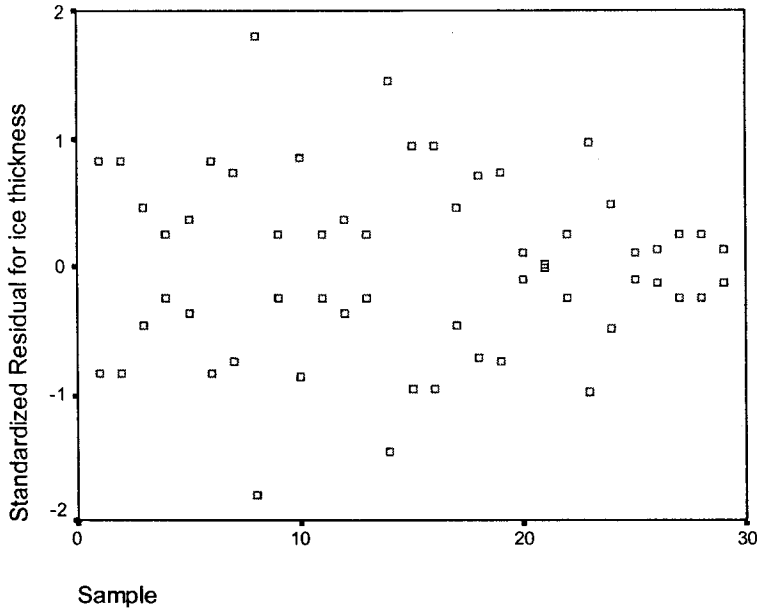

Fig. 36 Graph of standardized residuals versus foam sample

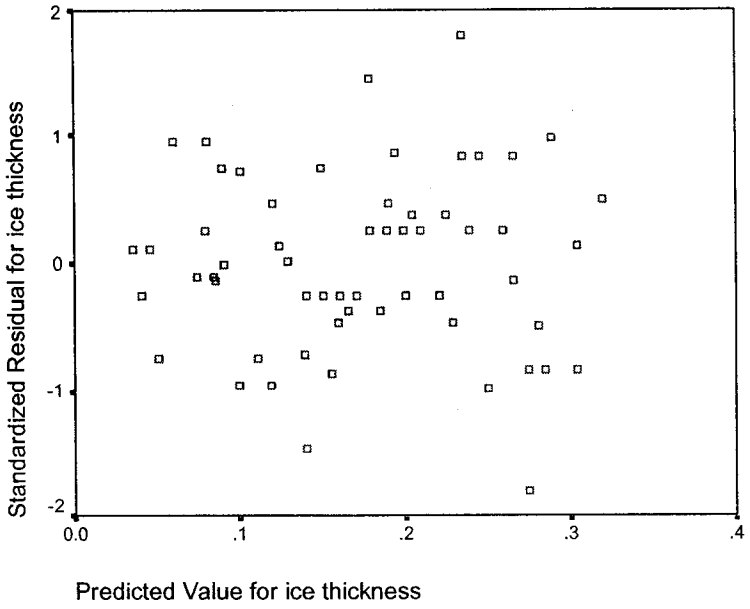

Fig. 37 Graph of standardized residuals versus predicted values

Figure 36 shows that the standard deviation or precision of the device over the range of the data does not vary. In other words, over the range of ice thicknesses used during testing, the precision was constant and not variable as noted by the manufacturer–MD Robotics.

Table 4 Correlation for Sample 1

	No. 1 Height	*No.1 MDR Ave.*
No. 1 Height	1	
No.1 MDR Ave.	0.820778	1

Table 5 Correlation for Sample 2

	No.2 Height Ave.	*No.2 MDR*
No.2 Height Ave.	1	
No.2 MDR	0.895192	1

Table 6 Correlation for Sample 7

	No.7 Height Ave	*No.7 MDR Ave.*
No.7 Height Ave	1	
No.7 MDR Ave.	0.991928	1

Table 7 Values and errors for Sample No. 7

Guage Height Ave (D)	MDR Ave(d)	absolute difference	relative difference
inches	inches	Abs(D-d)	Abs(D-d)/D
0.045	0.08	0.030	66.67
0.087	0.13	0.043	50.00
0.155	0.21	0.050	32.40
0.211	0.30	0.089	42.18
0.262	0.33	0.063	23.97

Sample No. 7 is probably the best sample to look at because it is the most homogeneous sample across each step. There is, on average, a 0.06 in. or 1.5 mm absolute error between the gauge measurements and MD Robotics camera measurements. Midvalues were used through out this table. This difference is twice the amount of experimental error in measurement of 0.03 in. or 0.7 mm.

Goodrich Corporation IceHawk System

System Operation

The second active system tested was a laser road surface sensor (LRSS) manufactured by the Goodrich Corporation of Minneapolis, Minnesota. This sensor system was designed to indicate the presence of ice or frost on roadways, with other models engineered to detect ice on aircraft surfaces. In operation, the IceHawk system scans a surface by transmitting a laser beam of polarized near-infrared light. Ice is detected by analyzing the polarization of the reflected signals. Where ice is present, the returned infrared signal is unpolarized. The images produced by the system are color-coded. Ice is displayed in red, snow in blue, and clean surfaces shown in gray. Surfaces that exhibit water are displayed in cyan. However, other objects such as plastic, fabric, grass, etc. may also be displayed in red, blue or light gray. Areas that do not receive enough signal return information are colored black.

The IceHawk LRSS is controlled remotely via a laptop computer, which is used to display and interpret road condition images. The LRSS consists of an optical ice detector mounted above and in close proximity to the surface of interest. When the LRSS performs a scan of the surface, data are saved in an image file on the hard drive of the LRSS. The image can then be downloaded to a computer, using Microsoft Windows 95™or 98™ operating systems using a RS-232 or modem interface.

System Testing

After contacting the company and obtaining the loan of a system for a three-week period, testing at TARDEC's VPL was conducted. The system tested was the next generation IceHawk wide-area ice detection system. This system was included for testing purposes because initial discussion with NASA-KSC representatives identified the IceHawk system and suggested that it be evaluated as part of this SOW.

To test the operating effectiveness with respect to distance, VPL investigators placed a large painted ET foam sample (provided by Goodrich) at varying distances (17, 30, 35, and 47 ft). These distances were chosen because of the space available in the lab. The IceHawk system requires that ET foam to be painted to increase light reflection and polarization for ice detection. The resolution seemed to get worse at greater distances, and the ice/frost delineation didn't improve. In a subsequent email conversation with a representative of the Goodrich Corp. (Tod Wollschlager), it was stated that the optics of the system could probably be modified, and a smaller laser spot size developed, to achieve the desired resolution.

TARDEC testing confirmed earlier somewhat unsuccessful testing results obtained by Goodrich in their Minneapolis facilities using NASA supplied ET foam samples. In this earlier test it was determined that ET foam did not provide the needed polarization effect needed to accurately measure ice thickness. The company does claim, however, that their systems are excellent in identifying clear ice on many surfaces–but that ET foam is a problem.

Test Results

It was noted with the current IceHawk system that thin ice is displayed as frost. The system also misidentifies non-ice/frost materials to be frost--like wood and diffusing materials. To test the frost/ice delineation, painted Sample No. 11 (as described earlier) was modified with machine screws (like Sample No. 1) to allow ice thickness to vary from $^{1}/_{16}$ to ¼ in.--top to bottom. Initially, IceHawk readings showed gray (defined as "clear" of ice) pixels in an upper middle region of the sample and red (ice) below. As time progressed (about 20 minutes), the gray area encompassed the top half of the sample with red in the bottom half. This change in color indicated that the system saw a change in ice thickness. However, it misreported the upper area as clear when ice was present.

It is thought that these false reading may have been associated with a pseudo-coloring problems, and something that Goodrich could adjust by software settings or further development. In subsequent e-mail conversations with Goodrich representatives, VPL investigators were told that the parameter data file (.cnf) could be adjusted to change the ice threshold level and other parameters. Concerning the scanned image improvement over time, it was noted that the ice surface seemed to be more opaque when first taken from the freezer. As the surface gradually became watery at room temperature, the ice became more transparent. This change may have affected measurement accuracy.

VPL investigators next moved the IceHawk system to an environmental chamber located at TARDEC. (See Figs. 38 and 39). The chamber had a region of frost, which accumulated on one of its walls, and the IceHawk system correctly characterized it as snow (blue). The density of this frost was not measured, but future frost tests would be appropriate. Figures 40 through 42 are the output images of the IceHawk system. *In summary, the IceHawk system tested is unable to determine the exact thickness of ice on an ET foam surface or frost.*

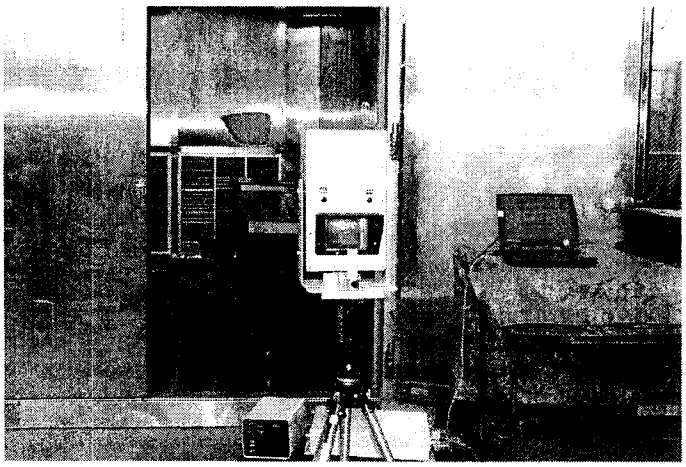

Fig. 38 View of chamber and ice from outside

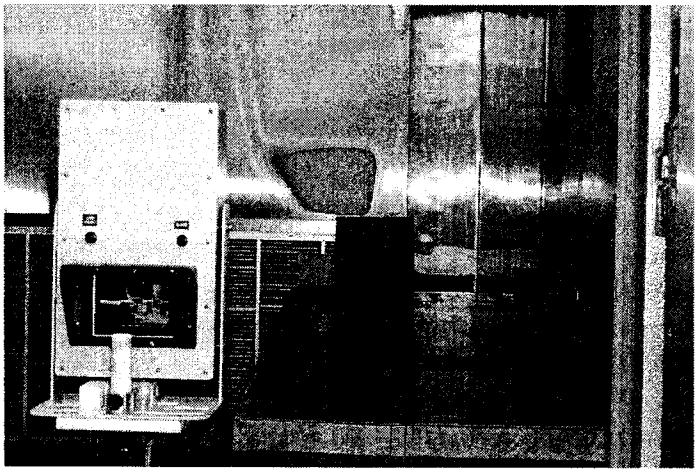

Fig. 39 Close-up of ice measured in chamber

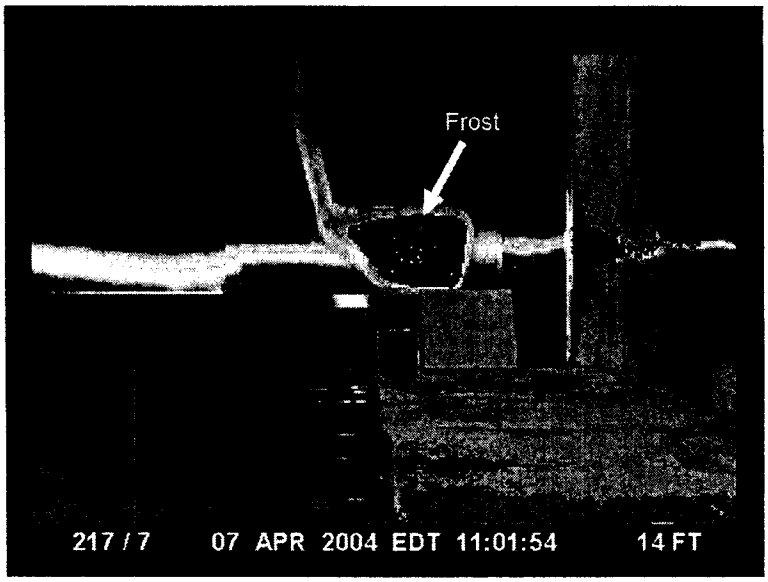

Fig. 40 IceHawk image of frost on chamber wall (two samples on table, left sample show frost incorrectly because of unpainted surface)

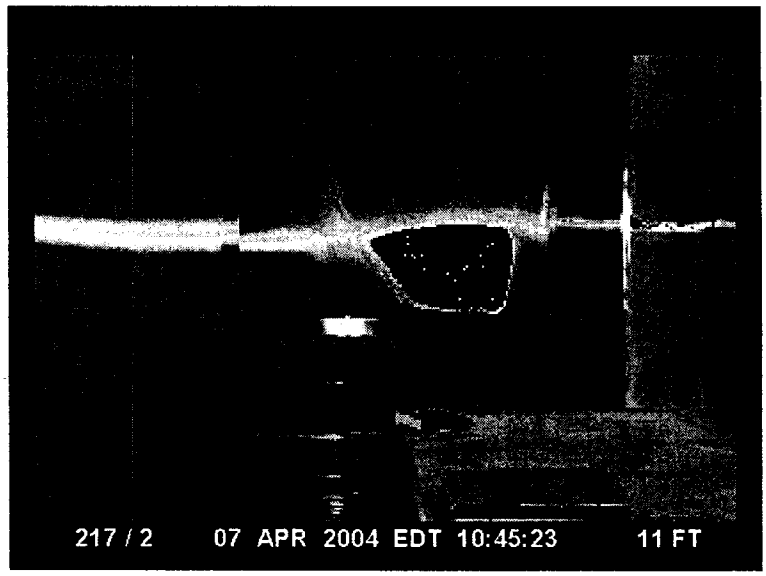

Fig. 41 IceHawk image 2 of ice/frost in an environmental chamber

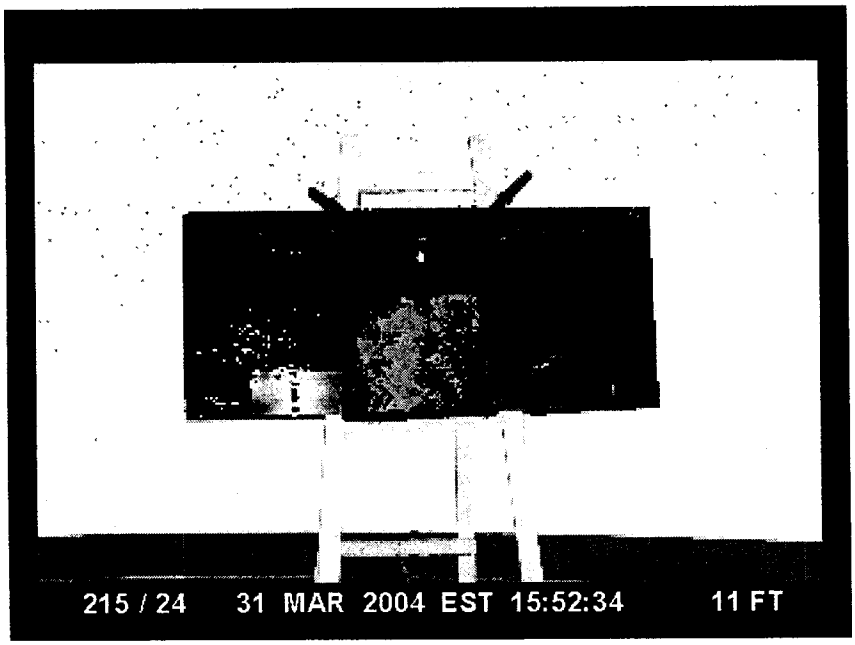

Fig. 42 IceHawk image of an ice covered ET foam sample in lab

Preliminary Conclusions

Neither of the two active systems (MD Robotics or IceHawk) tested in the U.S. Army's VPL produced the exact same measurements as a precision height gauge for simulated ET foam ice thickness. In addition, neither system accurately and reliably supported the pre-launch constraint for an ET ice thickness measurement limit of $1/16^{th}$ (0.0625) of an inch (in.), and the detection of ice having a diameter of not more that 1 in. --the primary objective of this SOW testing. However, there may be benefits to using either the Goodrich system or the MD Robotics system to detect the presence of clear ("black") ice because in some cases, ice on any part of the ET or Space Shuttle may be transparent and not visible to the naked eye.

More specifically, the MD Robotics system offers a promising approach for the approximate measurement of ice thickness in the presence of frost. The high correlation between the lab gauge readings and MD Robotics system measures is an indication that the physics of the method used is probably valid. There is a strong indication by the manufacturer that the system could be adjusted to meet the pre-launch constraints of ice thickness and size for pre-launch conditions given more time and development. However, since the ice thickness limit is of the same order of magnitude as the variability of the "bumpy" ET foam surface, this poses a problem for precision measurements, consistency, and confidence in the "go" or "no-go" launch decision process. While statistical analysis showed that there is a significant difference between the ice thickness determination of the MD Robotics system and height gauge measurements, this difference may not be of practical importance and within the range of acceptability for other ice/frost KSC applications. For example, the system could be used remotely to determine ice thickness over a certain area so that a relative comparison from time T_1 to time T_2 of ice growth or decline could be made to support an existing NASA ice growth model's predictions, or to supplement or provide input data to the model.

The Goodrich IceHawk system was found by VPL investigators to measure the presence of ice and frost under some conditions when the foam was painted. But the system as presently designed, does not provide accurate and quantitative measures of ice thickness on unpainted ET foam samples–a primary condition of this research effort. If only a presence determination of ice or frost on other more mechanical areas of the Space Shuttle or pad systems is needed such as LO2 bellows or supports, this system may be of value for future NASA pre-launch operations.

Suggestions for Future Research

There are several suggestions that can be made for future ET ice detection and measurement on existing samples using two active and one passive system, as well as a continued effort to find and test other commercially-available systems. TARDEC investigators will also continue to search scientific literature and the Internet for other potential systems for ice detection and measurement investigations. See Appendix B for possible Internet information source URLs. No further testing of the IceHawk system is planned because of the requirement that the foam surface is painted—an unlikely condition. Planned future investigation and testing includes systems and concepts by: (1) MD Robotic, (2) VE Tech/Canpolar Inc., and (3) TARDEC.

MD Robotics

Hopefully, MD Robotics will make their system (software and/or hardware modified) available for further testing in a lab environment to better determine the precision of the system and its independence of ice density. For future tests VPL investigators plan on simulating the conditions for growing low-density ice (frost) on ET foam samples in an environmental chamber located in Warren. Some simple calculations of the thermal conduction of ET foam based on its insulation characteristics from reported temperatures inside and outside surfaces have been made. Based on these calculations, a frost detection experiment could be designed to cool one side of a thinner section of an ET foam sample (about ¼ in.) using dry ice, to produce condensation-type frost on the outer foam surface. If the sample surface cannot be made cold enough using this approach, VPL investigators may attempt construction of a cryogenic tank apparatus testing with an available cryogen. Additional planned tests could help to validate the accuracy of the MD Robotics system and verify that reading is not affected by ice density.

VE Tech/Canpolar Incorporation

Plans are being developed to investigate and test additional sensor concepts and systems developed by VE Tech/Canpolar of St. John's Newfoundland, Canada. The purpose of this future test would be to determine its value for ET frost/ice detection and measurement. This active system is based on the low power laser technique illustrated earlier in Figs. 16, 17, and 18. This system makes use of the principle of total internal reflection to measure ice thickness remotely.

TARDEC Image Fusion

Future TARDEC VPL work is also planned to investigate the use of a passive system for ice detection and thickness determination using a sensor fusion concept. One possibility is the use of a technique of the addition or subtraction of several bands of the IR spectrum obtained from a multi-band Charged Coupled Device (CCD) camera and infrared camera data. These sensors would be used in conjunction with Sarnoff image processing boards to perform image and data addition and subtraction much like logic circuits in a computer. Since the refractive index of ice is wavelength dependent (see Fig. 43), this physical characteristic should be of value for imaging and ice thickness determination.

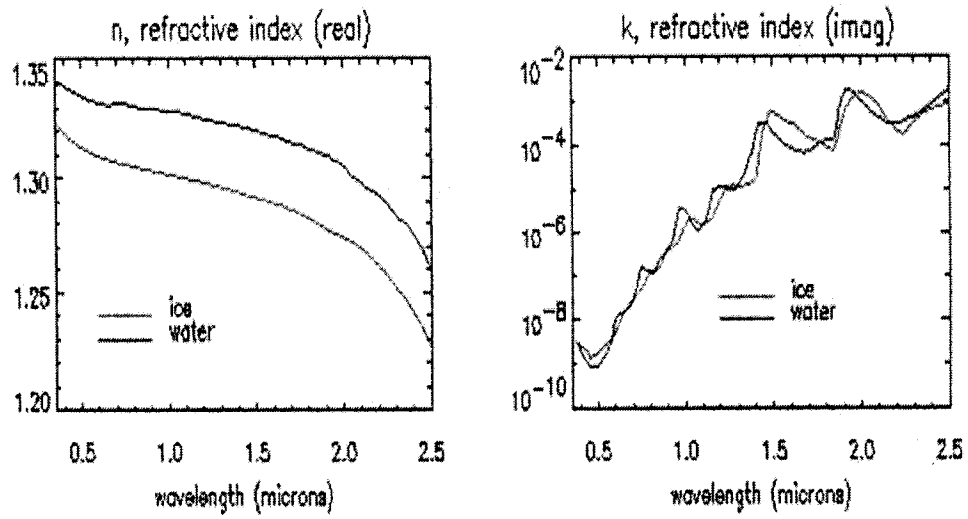

Fig. 43 Wavelength dependence of the real and imaginary parts of the refractive index

References

1. Email communication from Mr. Armando Oliu, NASA Ice/Debris Team Leader, March 3, 2004.
2. National Aeronautics and Space Administration (NASA). Lyndon B. Johnson Space Center. Ice/Debris Inspection Criteria NSTS 08303 Revision A. Houston, Texas: 1991.
3. Hermanto, I., Gagnon, R.E., "Machine Vision for Ice Layer Thickness Measurements", http://www.campolar.com.
4. Yankielun, N.E., Ryerson, C.C., Jones, S.L., "Wide-Area Ice Detection Using Time Domain Reflectometry", Technical Report ERDC/CRREL TR-02-15, Oct. 2002.
5. Montgomery, D.C., *Design and Analysis of Experiments*, 4th Ed., John Wiley & Sons, New York, New York, 1977, pgs. 475-478.
6. DeAnna, R.G., Mehregany, M., Roy, S., Zakar, E., " Microfabricated ice-detection sensor", SPIE Smart Structures and Materials Conference, San Diego, CA, March 2-6, 1997.

Appendix A

Abbreviations

CCD: Charge Coupled Device
ET: External Tank
FSS: Fixed Service Structure
GOX: Gaseous Oxygen (GO2)
IR: Infrared
LCC: Launch Commit Criteria
LH2: Liquid Hydrogen
LO2: Liquid Oxygen
LRSS: Laser Road Surface Sensor (by Goodrich Corporation)
SOFI: Spray-on Foam Insulation
SOW: Statement of Work
SRB: Solid Rocket Booster
SSME: Space Shuttle Main Engine
SSP: Space Shuttle Program
TPS: Thermal Protection System
TSE: Transportation Support Equipment
VAB: Vehicle Assembly Building
XT X-Axis of External Tank
YT: Y-Axis of External Tank
ZT: Z-Axis of External Tank

Appendix B

Sensor Technology Websites

http://www.idiny.com/abstracts/ssi.html
http://www.vibro-meter.ch/aerospace/ice.html
http://www.pennyandgiles.com/products/products.asp?strAreaNo=402_15
http://www.photonics.com/spectra/business/XQ/ASP/businessid.317/QX/read.htm

Appendix C

Table C.1 Data recorded of ice thickness

Sample #	Area	Foam Thickness						Average			Actual measure: Ice + Foam			Actual measure: Ice Thickness			MDR	MDR
	NE C	1.5									1.783			0.283			0.23	0.27
	NW C	1.48									1.775			0.295			0.25	0.29
1	SE C	1.42									1.63			0.21			0.18	0.24
1/16-1/4"	SW C	1.48									1.612			0.132			0.16	0.21
ramp	Center	1.52									1.685			0.165			0.22	0.26
	Bump	1.59																
	Chip	1.29																
																		2nd
	Mid 1																	0.35
	Mid 2																	0.32
	Mid 3																	0.27
	Mid 4																	0.24
	Mid 5																	0.19
	NE C	1.48									1.748			0.268			0.24	
	NW C	1.525									1.547			0.022			0.12	
2	SE C	1.425									1.736			0.311			0.2	
1/32-1/4"	SW C	1.499									1.533			0.034			0.09	
	Center																0.17	
		Bottom(1)	Bottom (2	Mid(1)	Mid(2)	Top(1)	Top (2)	Bottom	Mid	Top	Bottom	Mid	Top	Bottom	Mid	Top	Mid	
molded step	St 1		1.433				1.477	1.433	No reading	1.477	1.736		1.748	0.303	No reading	0.271	0.23	
	St 2		1.566				1.498	1.566	No reading	1.498	1.675		1.692	0.109	No reading	0.194	0.22	
	St 3		1.541				1.43	1.541	No reading	1.43	1.621		1.631	0.08	No reading	0.201	0.18	
	St 4		1.576				1.484	1.576	No reading	1.484	1.565		1.576	-0.011	No reading	0.092	0.13	
	St 5		1.503				1.517	1.503	No reading	1.517	1.533		1.547	0.03	No reading	0.03	0.09	
	NE C	1.511									1.633			0.122			0.23	
	NW C	1.431									1.624			0.193			0.25	
3	SE C	1.497									1.644			0.147			0.22	
3/16" nuts	SW C	1.475									1.63			0.155			0.22	
	Center	1.578									1.658			0.08			0.24	
	Bump																	
	Chip																	
	NE C	1.41									1.511			0.101			0.06	
	NW C	1.34									1.464			0.124			0.08	
5	SE C	1.43									1.57			0.14			0.14	
1/8" snow	SW C	1.43									1.555			0.125			0.11	
NW rough	Center	1.46									1.561			0.081			0.18	
	Bump	1.52															0.17	
	Hole	1.29															0.22	
	NE C	1.263									1.267			0.004				
	NW C	1.261									1.265			0.004				
7	SE C	1.262									1.268			0.006				
Milled steps	SW C	1.265									1.278			0.013				
	Center										1.27							
		Bottom(1)	Bottom (2	Mid(1)	Mid(2)	Top(1)	Top (2)	Bottom	Mid	Top				Bottom	Mid	Top	Mid	Top
	St 1-avg	1.225	1.22	1.223		1.227	1.227	1.2225	1.223	1.227	1.27			0.045	0.047	0.043	0.08	0.07
	St 2-avg	1.178	1.175	1.184		1.188	1.188	1.1765	1.184	1.188	1.27			0.092	0.086	0.082	0.13	0.13
	St 3-avg	1.105	1.104	1.116		1.126	1.123	1.1045	1.116	1.1245	1.27			0.165	0.154	0.1455	0.21	0.2
	St 4-avg	1.052	1.048	1.061		1.062	1.066	1.05	1.061	1.064	1.27			0.218	0.209	0.206	0.33	0.27
	St 5-avg	1.002	1.003	1.007		1.014	1.015	1.0025	1.007	1.0145	1.27			0.268	0.263	0.2555	0.34	0.31
	NE C										1.236			1.236				
	NW C										1.227			1.227				
8	SE C										1.244			1.244				
molded step	SW C										1.233			1.233				
		Bottom(1)	Bottom (2	Mid(1)	Mid(2)	Top(1)	Top (2)	Bottom	Mid	Top							Mid	Top
milled flat	St 1-avg		1.232				1.231	1.232	No reading	1.231	1.235			1.235			0.04	0.02
snow	St 2-avg		1.221				1.225	1.221	No reading	1.225	1.235			1.235			0.13	0.11
	St 3-avg		1.218				1.225	1.218	No reading	1.225	1.235			1.235			0.21	0.18
	St 4-avg		1.222				1.225	1.222	No reading	1.225	1.235			1.235			0.24	0.23
	St 5-avg		1.228				1.234	1.228	No reading	1.234	1.235			1.235			0.23	0.23
	NE C										1.386			1.386				
	NW C										1.33			1.33				
9	SE C										1.407			1.407				
molded step	SW C										1.406			1.406				
		Bottom(1)	Bottom (2	Mid(1)	Mid(2)	Top(1)	Top (2)	Bottom	Mid	Top							Mid	Top
snow	St 1-avg		1.414				1.411	1.414	No reading	1.411				0			0.07	0.02
	St 2-avg		1.371				1.401	1.371	No reading	1.401				0			0.12	0.11
	St 3-avg		1.342				1.369	1.342	No reading	1.369				0			0.18	0.19
	St 4-avg		1.367				1.359	1.367	No reading	1.359				0			0.21	0.22
	St 5-avg		1.381				1.351	1.381	No reading	1.351				0			0.23	0.24
	NE C										1.29			1.29			0.07	
	NW C										1.41			1.41			0.16	
10	SE C										1.327			1.327			0.18	
1/4-1/2"	SW C										1.424			1.424			0.19	
snow	Center													0			0.26	
	Bump													0			0.14	
	Chip													0				
		1		(2)														
	NE C	1.429		1.41										-1.429			0.14	
	NW C	1.307		1.281										-1.307			0.16	
11	SE C	1.354		1.328				1.0788						-1.354			0.11	
painted	SW C	1.304		1.303										-1.304			0.15	
	Center	1.435		1.413										-1.435			0.09	
	Bump																	
	Chip																0.1	
	NE C																0.19	
	NW C																0.14	
Large	SE C																0.27	
Piece	SW C																0.03	
12"*12"	Center																0.15	
		Bottom(1)	Bottom (2	Mid(1)	Mid(2)	Top(1)	Top (2)											
	Mid 1																0.19	
	Mid 2																0.18	
	Mid 3																0.14	
	Mid 4																0.17	
	Mid 5																0.17	

Appendix D

Fowler Height Meter

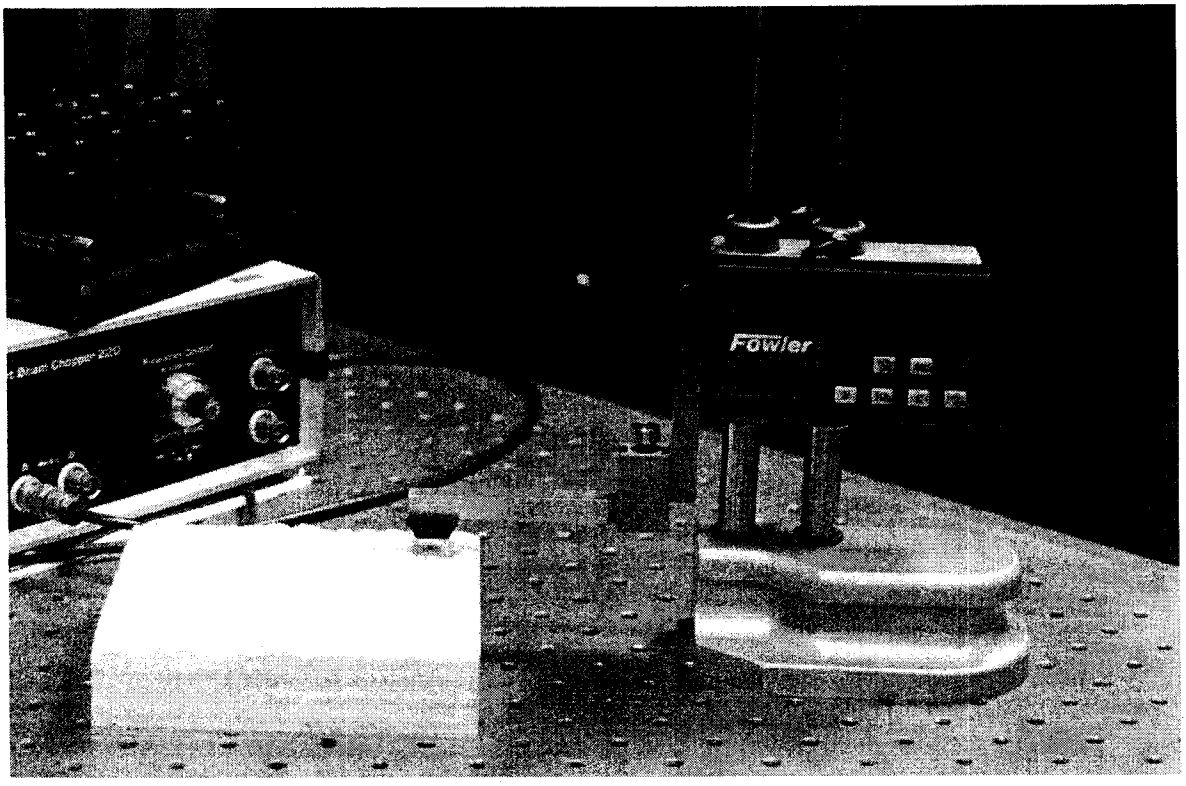

Fig. D.1. Fowler Height Gauge